Ground motion measurement in the Lake Mead area, Nevada, by differential SAR interferometry time series analysis: Probing the lithosphere rheological structure

Doin, M.-P., Cavalié, O., Lasserre, C.

Laboratoire de Géologie, UMR8536,
Ecole Normale Supérieure
Paris

How does the crust and uppermost mantle respond to stress at short time scale ?

Elastic response At least for time scales up to 1 year

Visco-elastic response

* Post-glacial rebound : ~3000 years.
  Mean mantle viscosity 10^{21} Pa.s
  $\tau \sim \eta\ k / \rho g$
  Depth + lateral variations of viscosity
* Isostatic rebound of palaeo-lakes
  Lake Bonneville, Lake Lahontan
  300 years,
  viscosity of 4×10^{17} to 10^{19} Pa.s
* Post-seismic rebound:
  transient rheologies with low viscosity

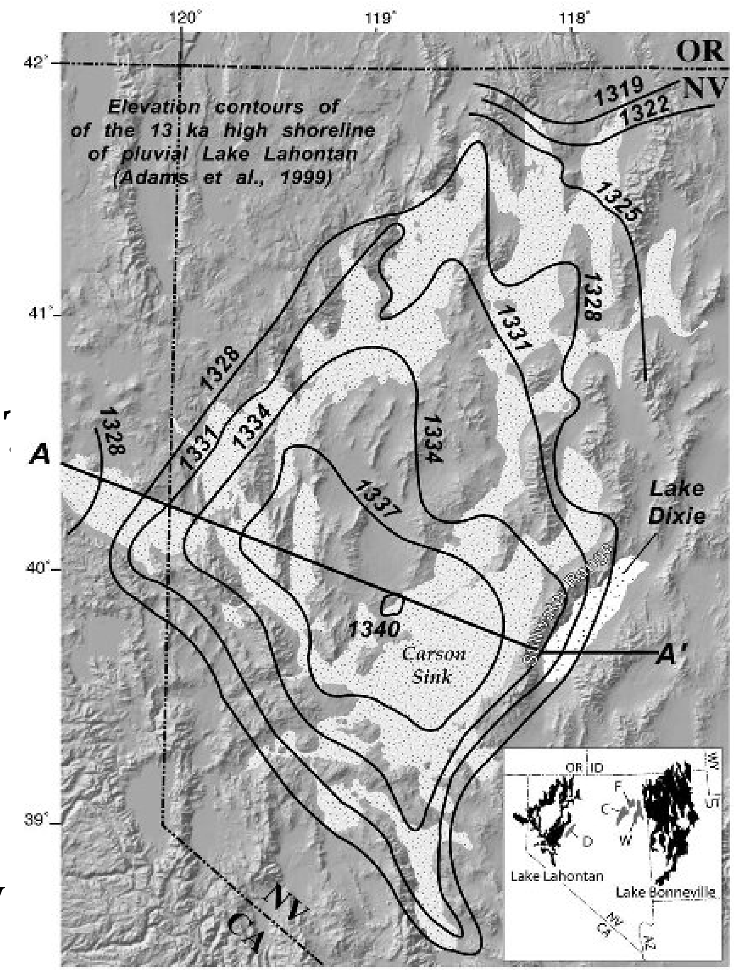

Shorelines elevation, Lake Lahontan
Adams et al., 1999

Surface load : Lake Mead water level fluctuations

In the Basin and Range,
Nevada, Arizona, USA :

- thin lithosphere
- desert

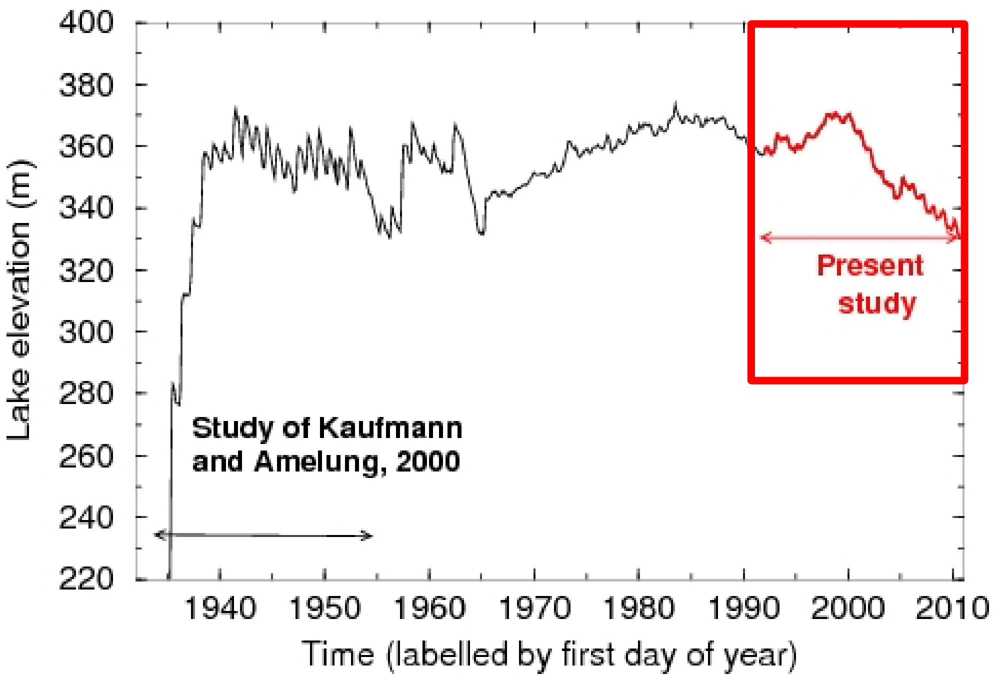

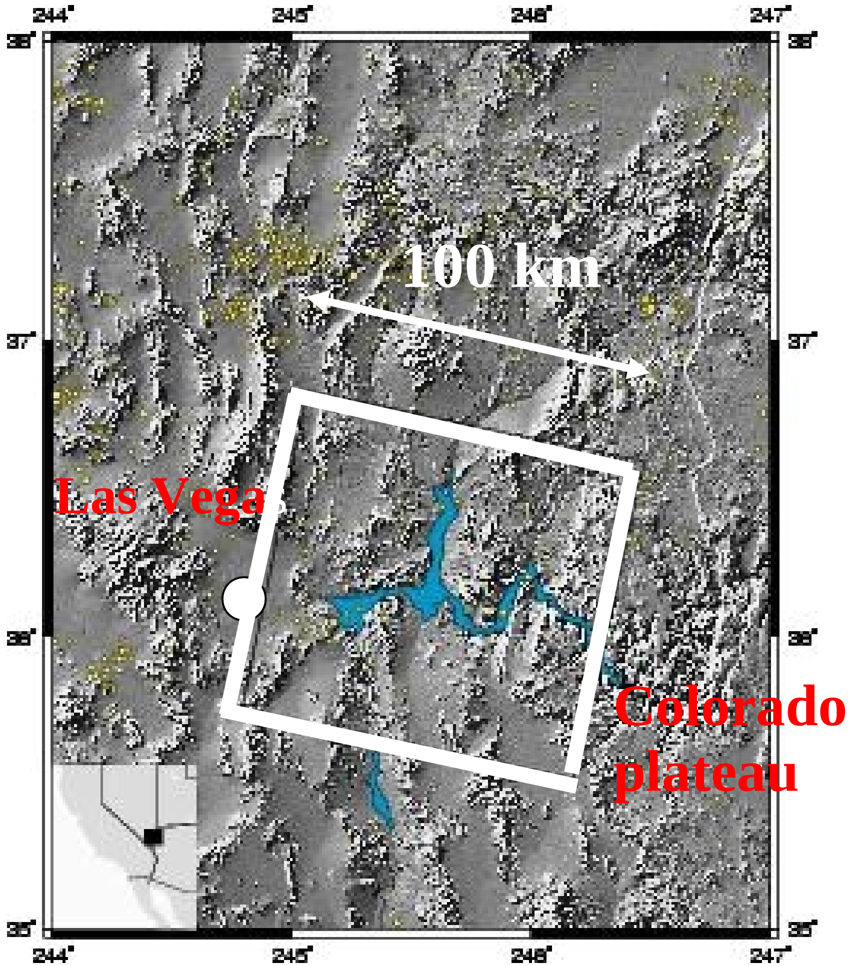

Study of Kaufmann and Amelung (2000) : 1935-1965

- Impoundment in 1935 was followed by a delayed subsidence : 17 cm between 1935 and 1950 *(Longwell, 1960)*

- Elastic thickness : 32 km

Mantle viscosity : 10^{18} Pa s

Relaxation time : 25 yrs

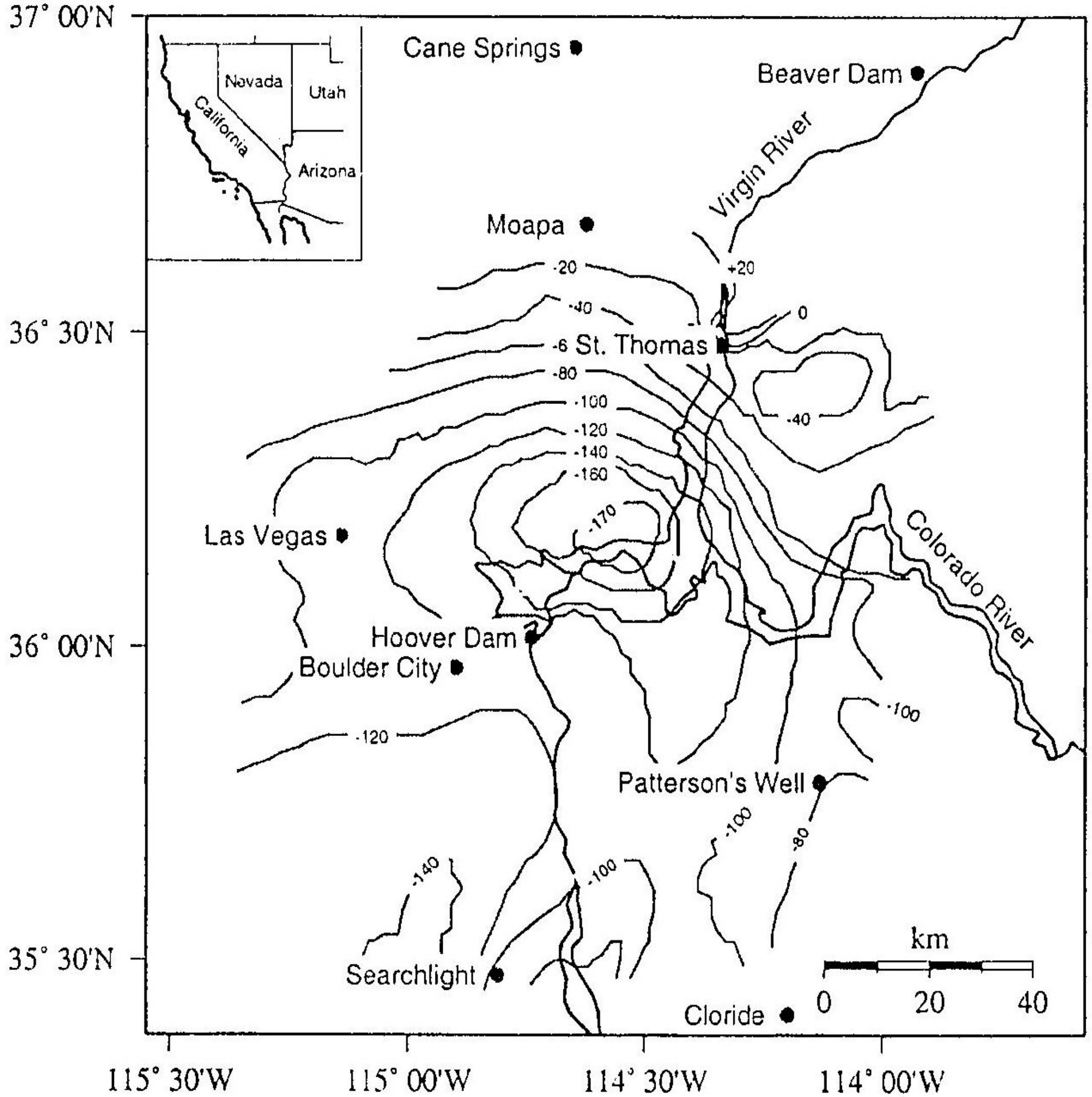

Subsidence map derived from leveling surveys results

SAR data : 63 ERS acquisitions, 45 Envisat acquisitions
analysed with a Small BASeline approach (Schmidt and Bürgmann, 2003)

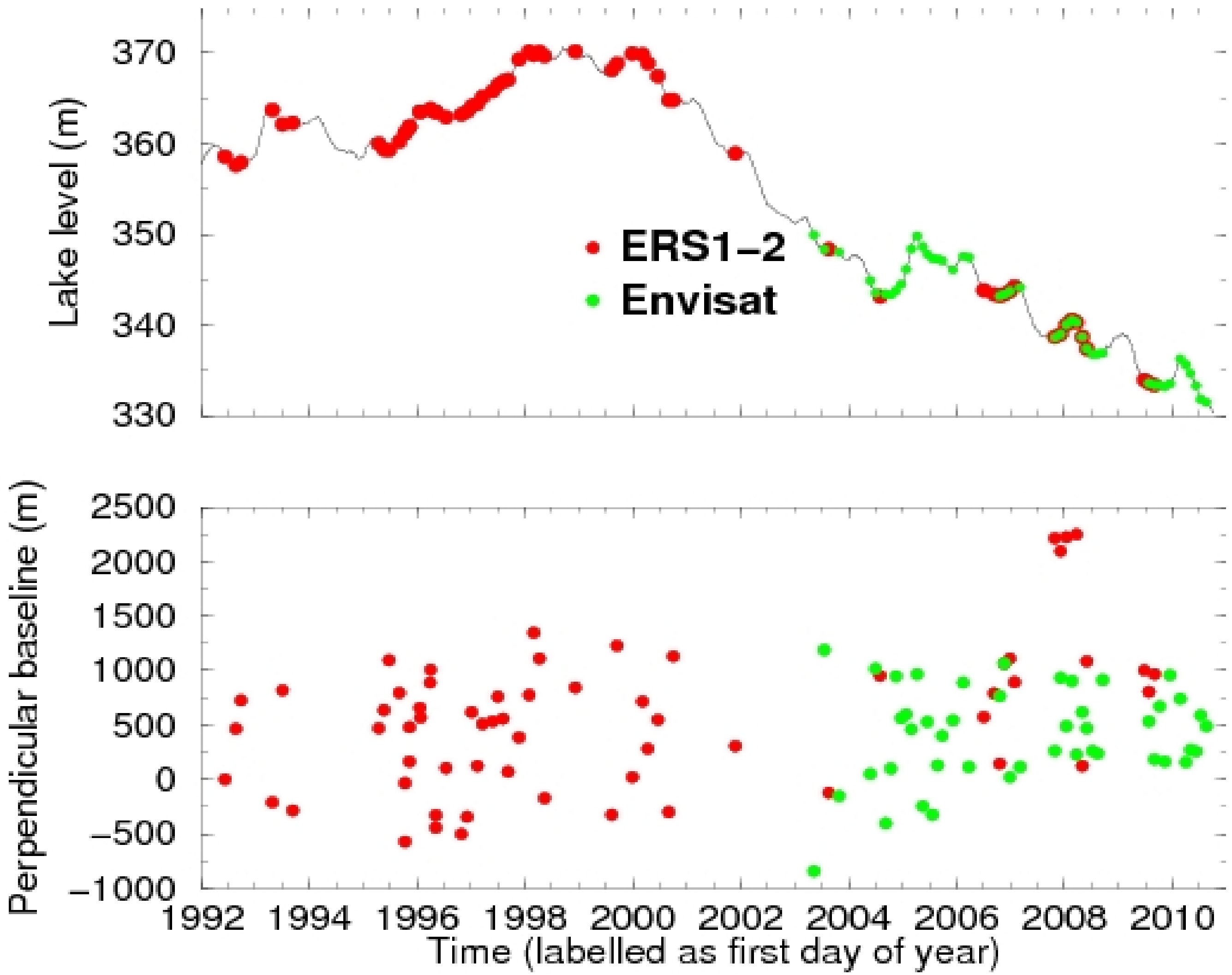

553 interferograms : very high network redundancy

ERS (pre-2001)-ERS(post 2002) interferograms :

1996-03-30 to 2006-11-19 : water decline by 20 m, up to 2.5 cm of uplift

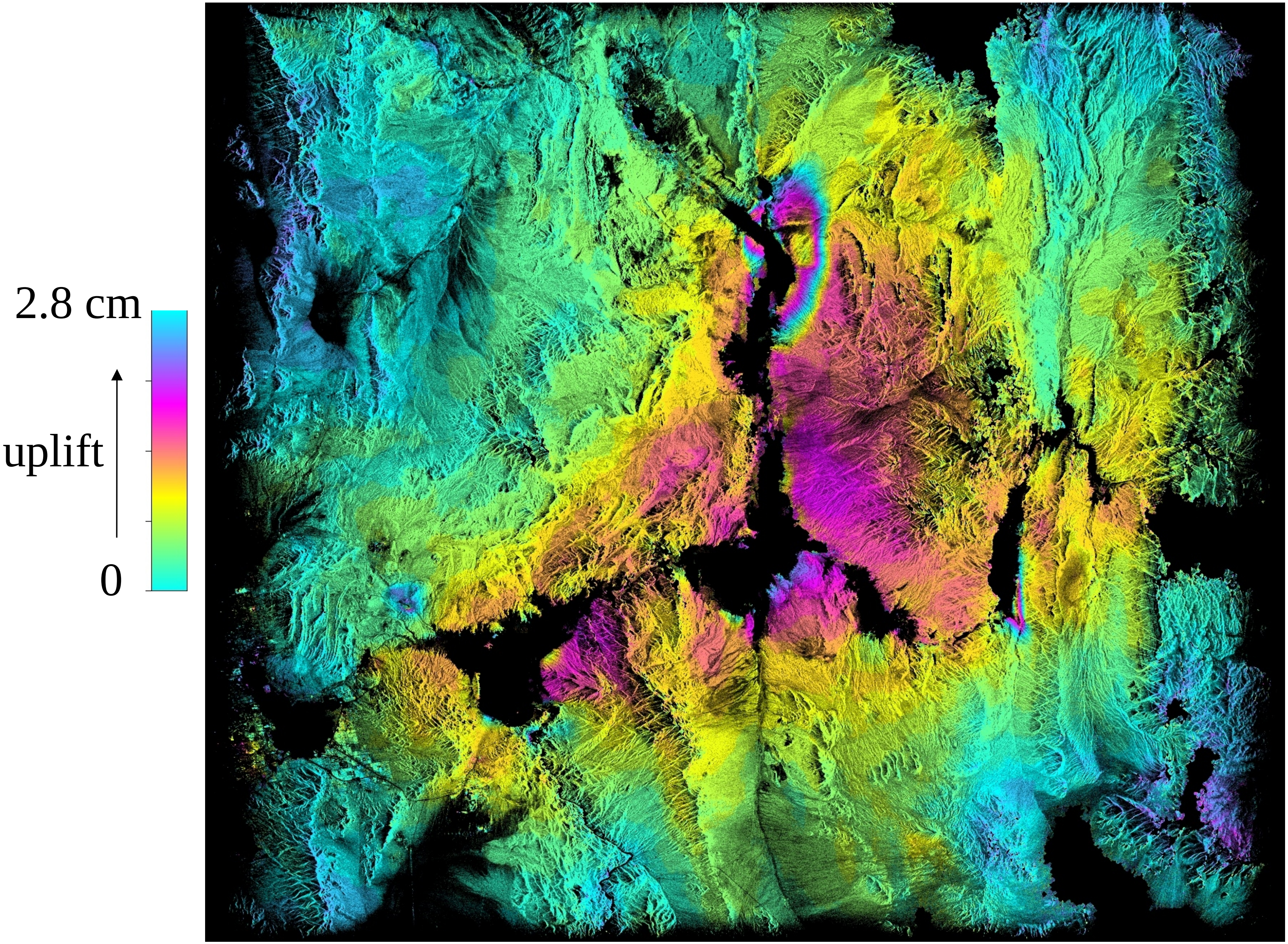

553 Differential SBAS interferograms

= Orbit error (~ 5 cm) + Atmospheric delays (~4 cm) + ground motion (~2 cm) + noise

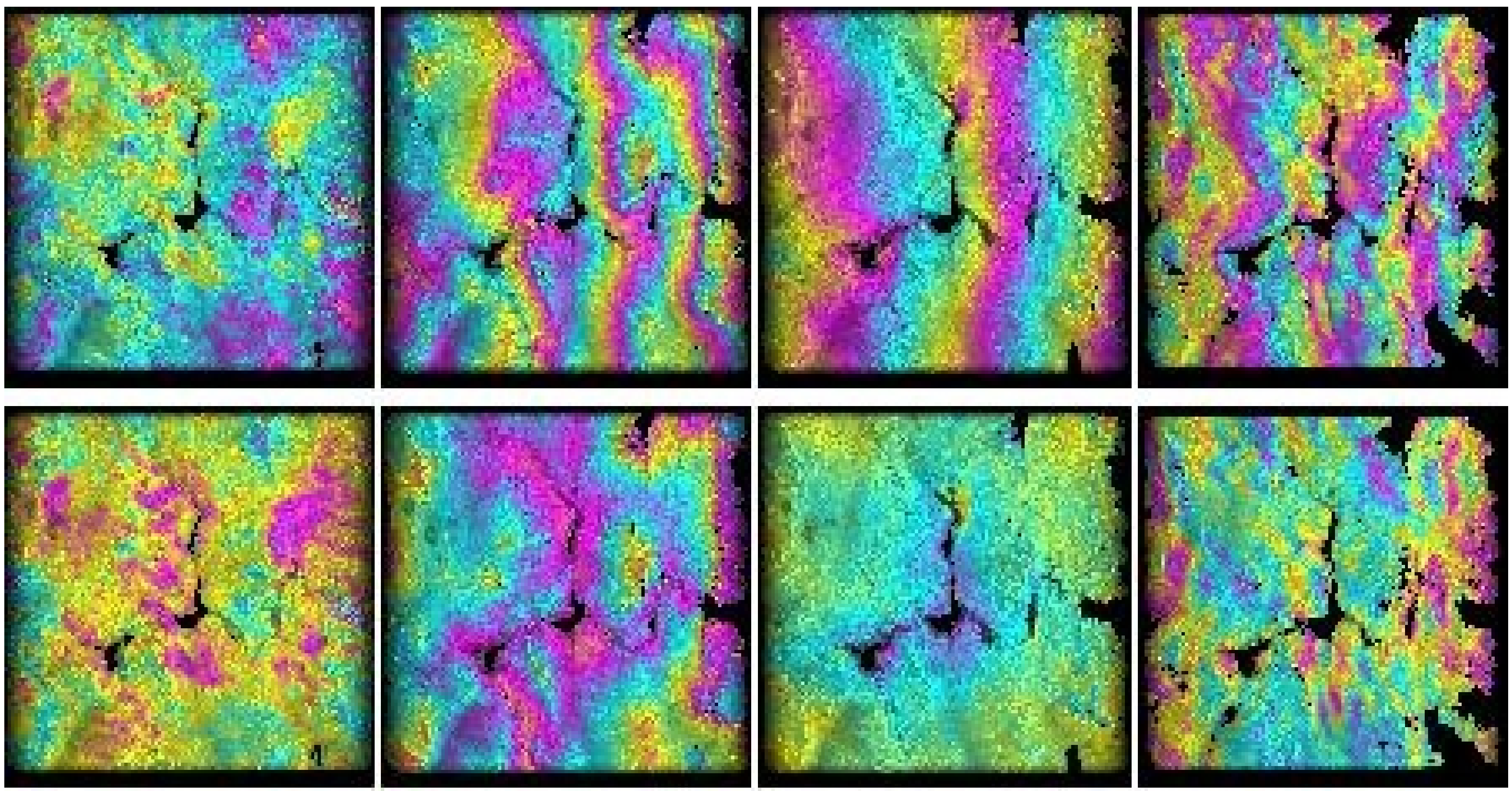

(a) 1995/04/05-1997/03/16 (b) 1995/11/12-1997/01/15 (c) 1996/01/20-1998/01/25 (d) 1997/02/09-2001/11/25

Remove "twisted" plane

Atmospheric delays : Phase-elevation correlation

Interferogram

DEM

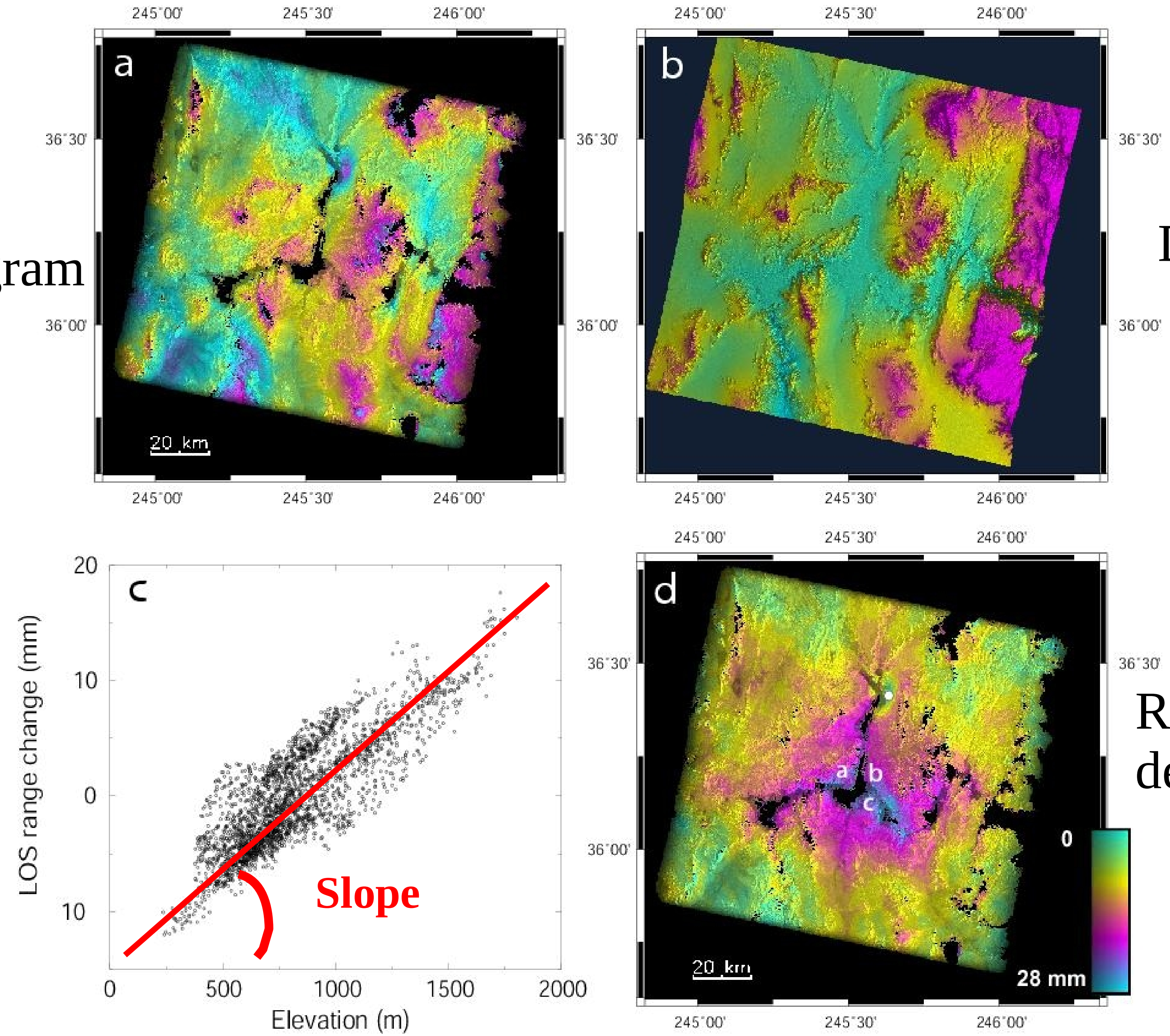

Residue : deformation

Phase-elevation correlation : comparison with predictions derived from the North American Regional Analysis

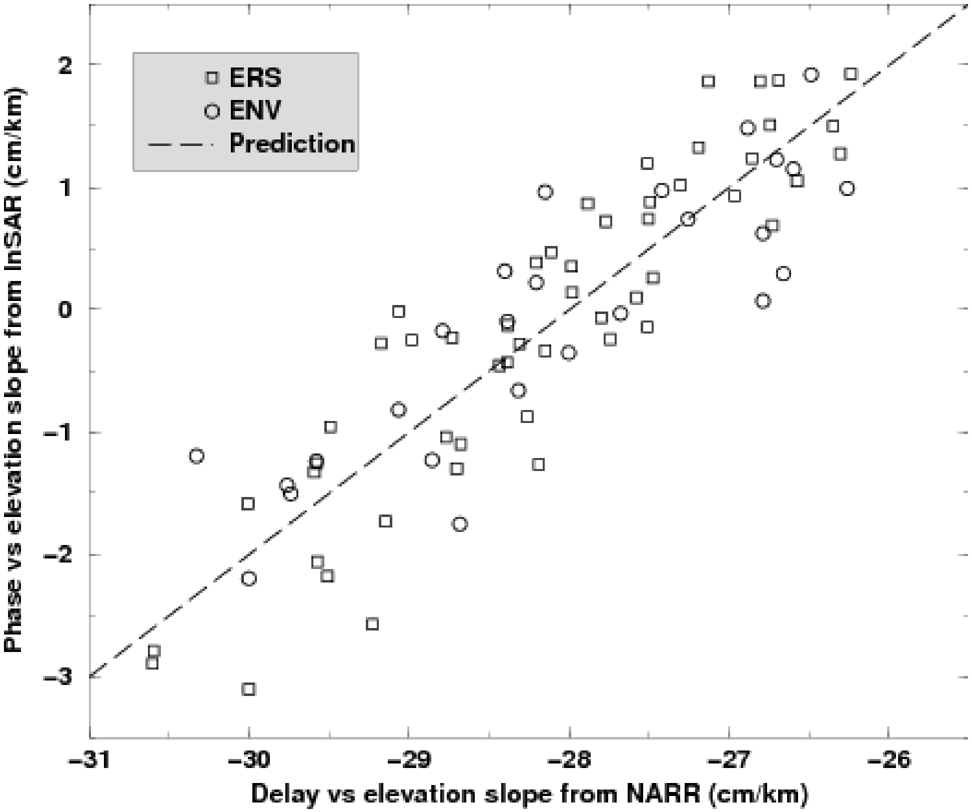

COMPARISON
DInSAR
versus
NARR prediction

Doin et al.,
J. of Applied
Geophys., 2009

Random patterns

Ripples, bubbles, patches, fronts, ...

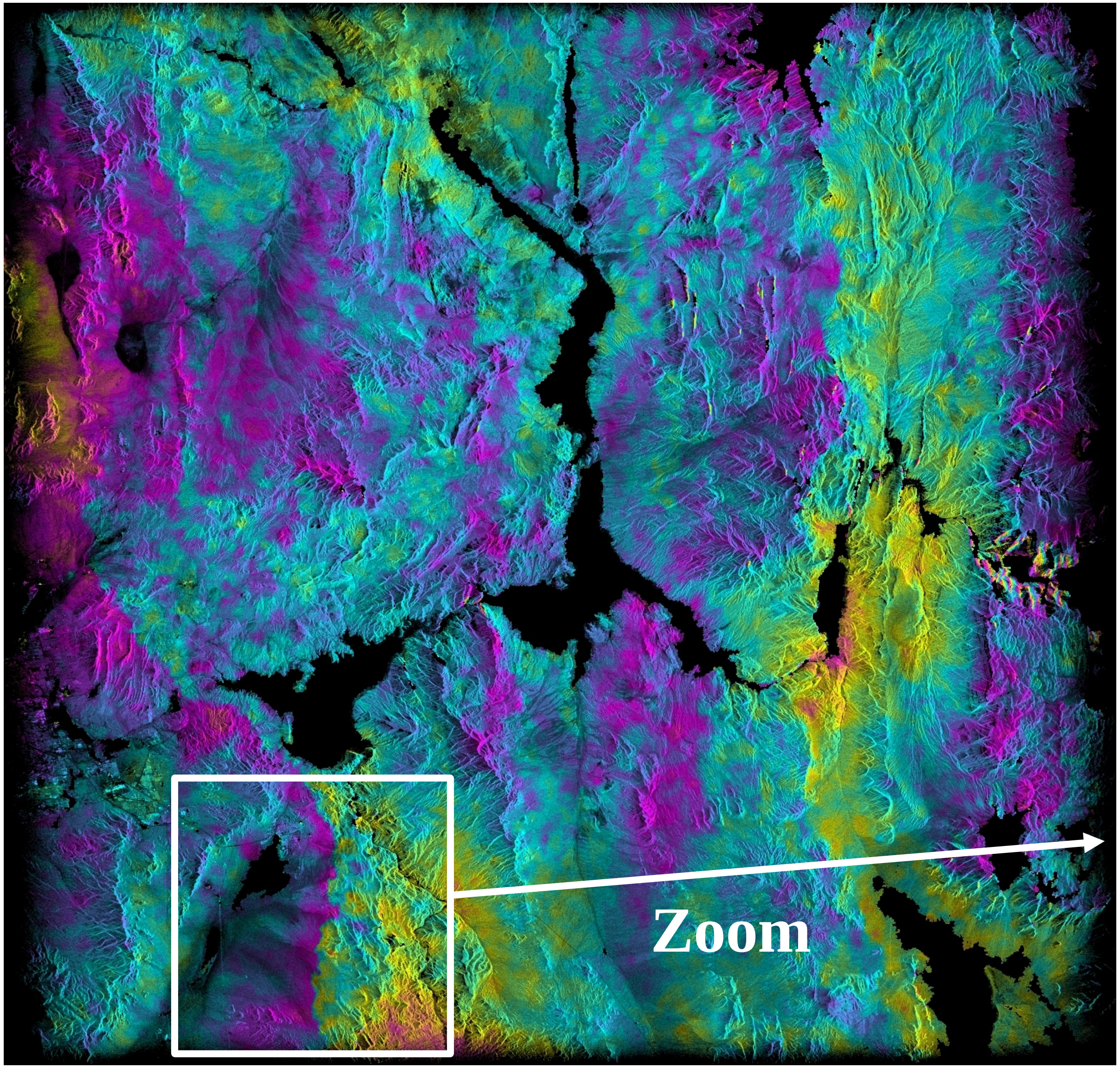

1992-08-20 1995-04-15
1 color cycle = 5.6 cm

1 color cycle = 2.8 cm

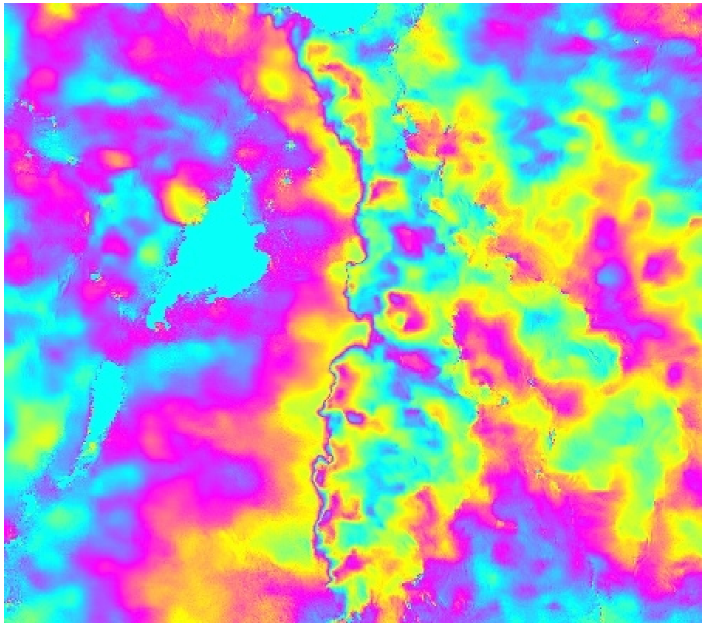

Random patterns : compute structure functions for each interferogram

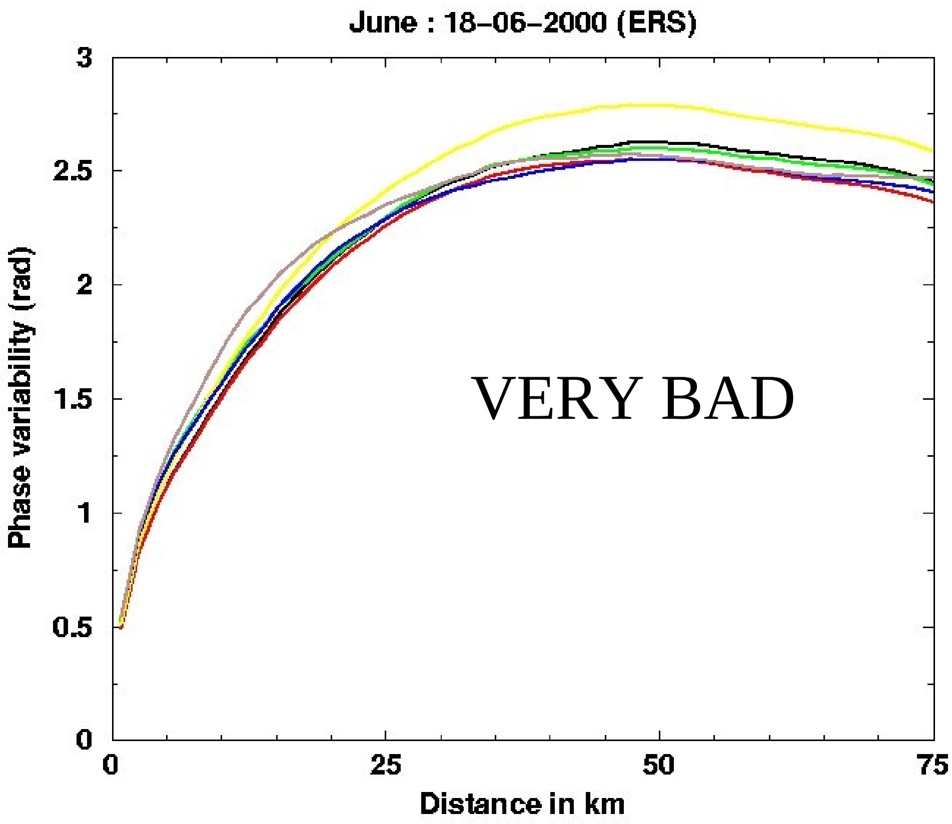

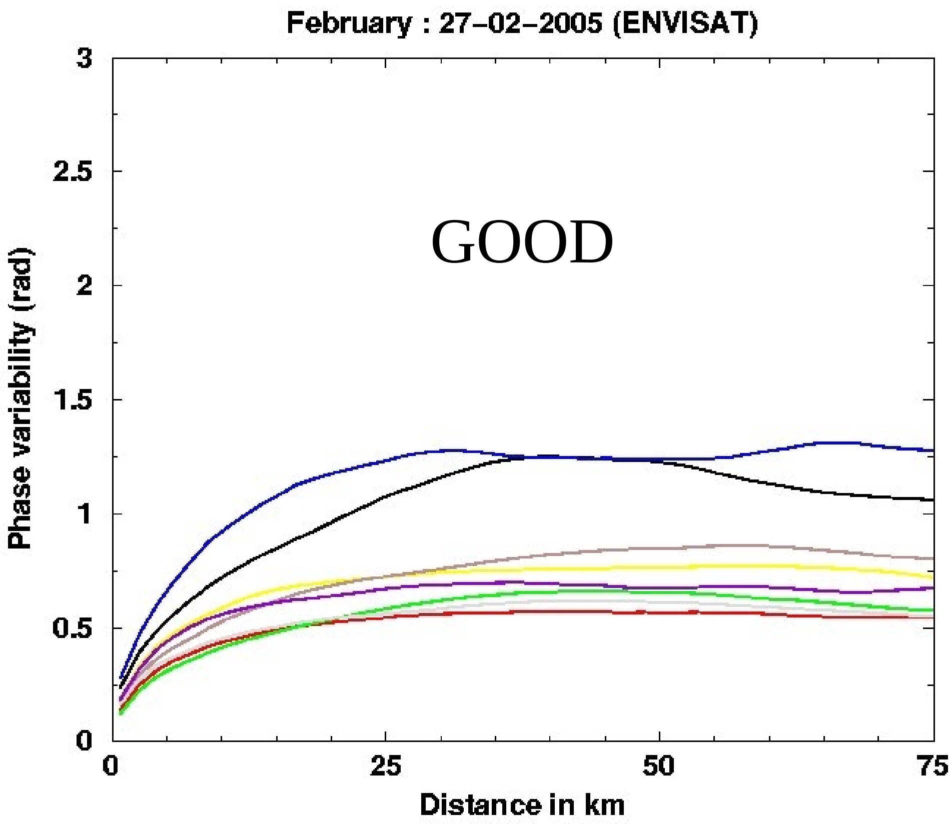

==> After network inversion:
Amplitude of turbulent atmosphere (APS) for each date

Inversion of interferograms into time series

- Use 553 corrected interferograms based on 107 acquisitions, invert for successive increments of phase delays
- Check for unwrapping errors using the strong interferometric network redundancy and correction
- Link the ERS and Envisat time series by adjusting the phase of acquisitions 30 min apart
- Invert the DEM error and correct the phase of each acquisition accordingly

==> Time series of raw phase delay maps at each acquisition date (including mainly deformation and turbulent atmosphere)
==> Smoothed time series which contains mostly deformation

Separation of signals : atmosphere / hydrology / effect of water load

Smoothed time series : mainly deformation

Raw phase delay: turbulent atmospheric patterns + deformation

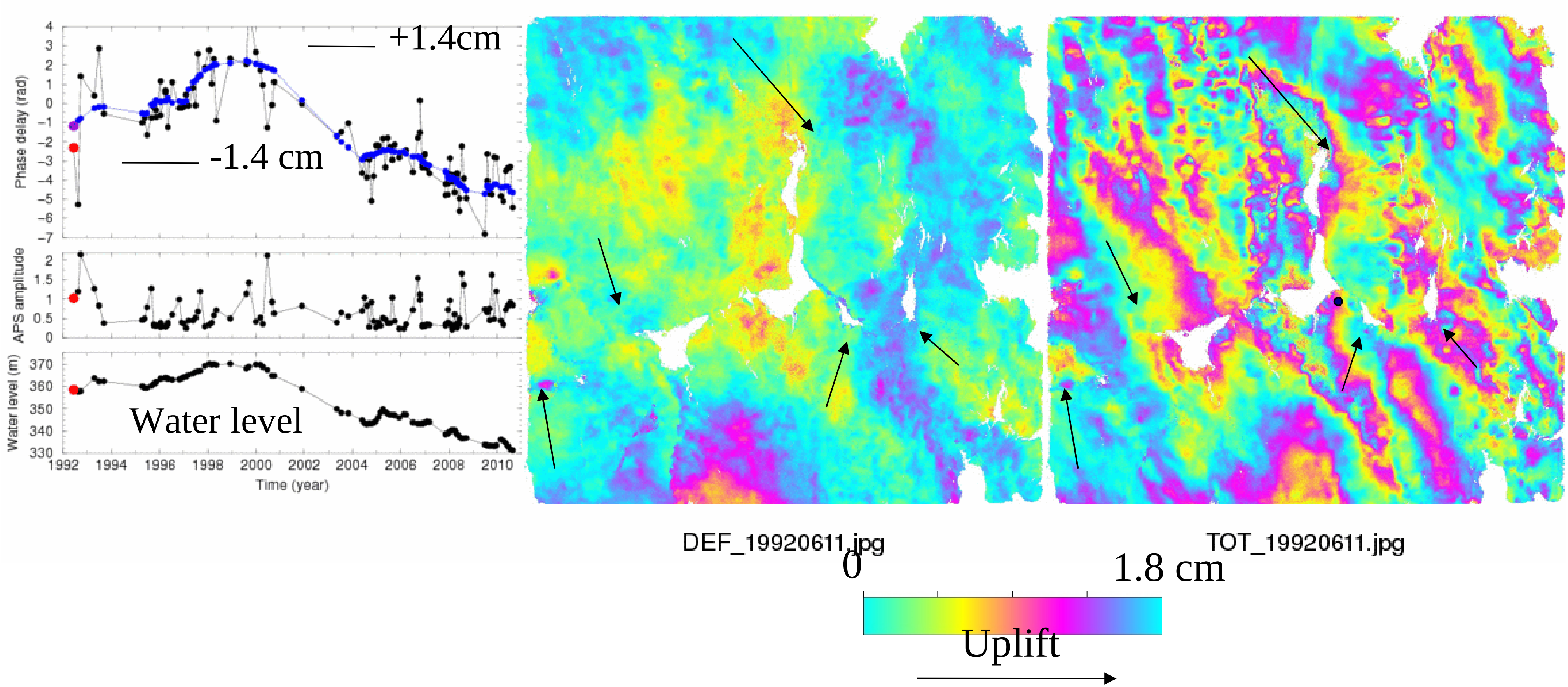

Smoothing weighted by the amplitude of atmospheric patterns

Separation of signals : Principal Component Analysis

First eigen vector:

On raw phase delays

On smoothed phase delays

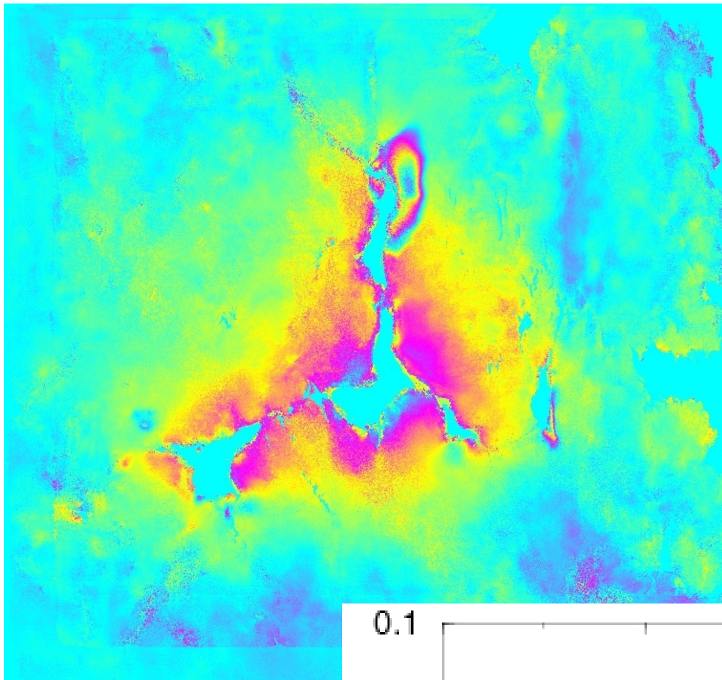

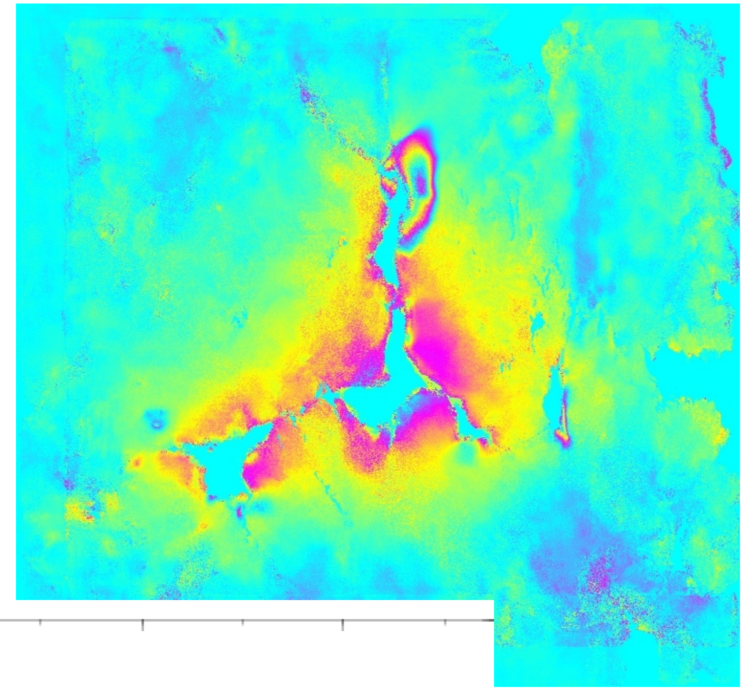

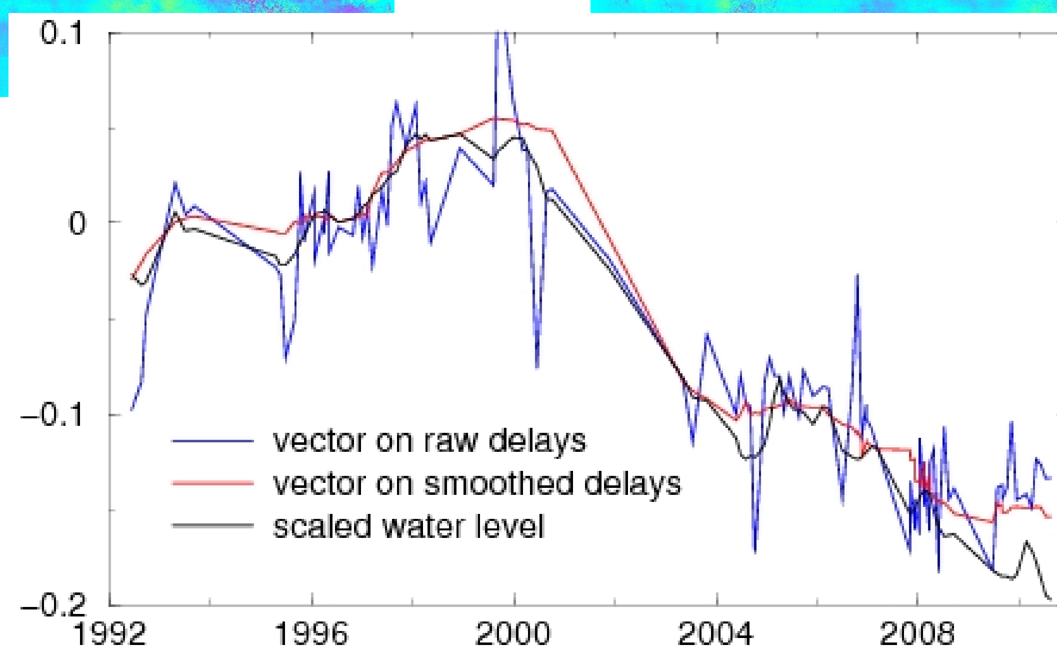

Separation of signals : Principal Component Analysis

Following eigen vectors on smoothed phase delays

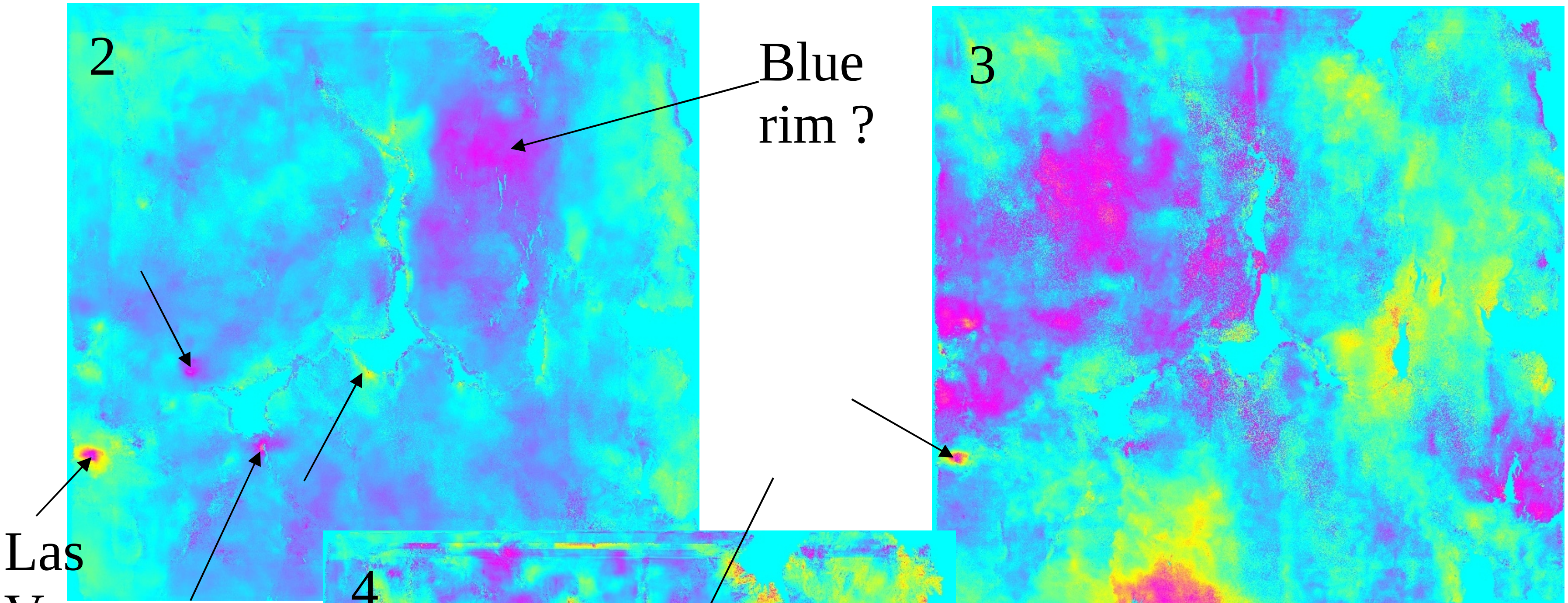

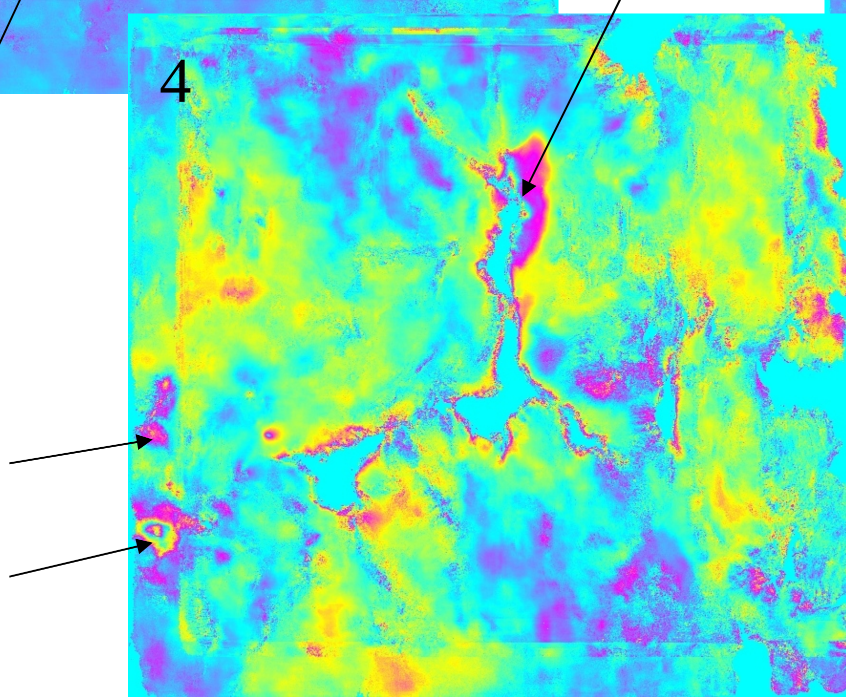

Physical interpretation ?

Hydrological signals :

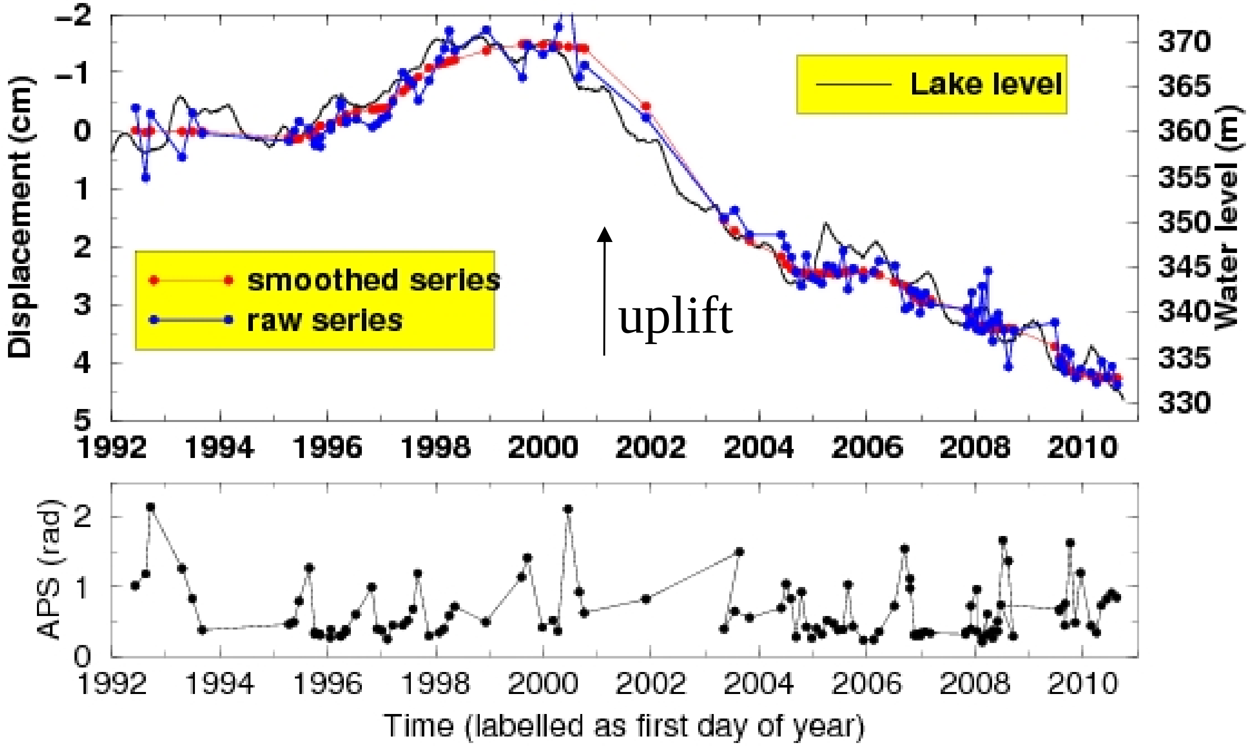

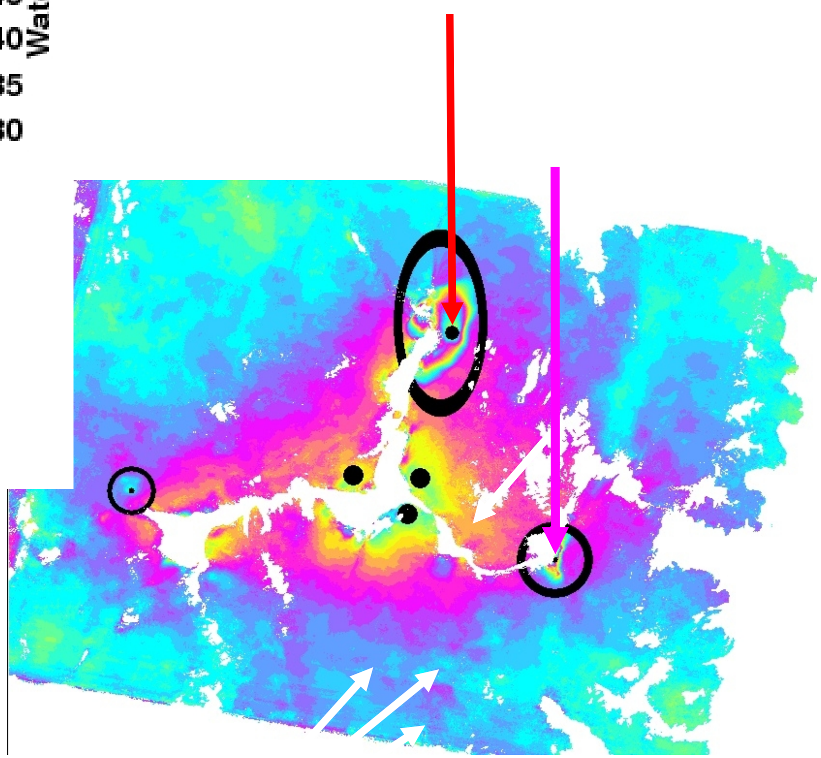

~3months delay between ground motion and lake level change : water diffusion

Regression coefficient between data and lake level

Hydrologic signals

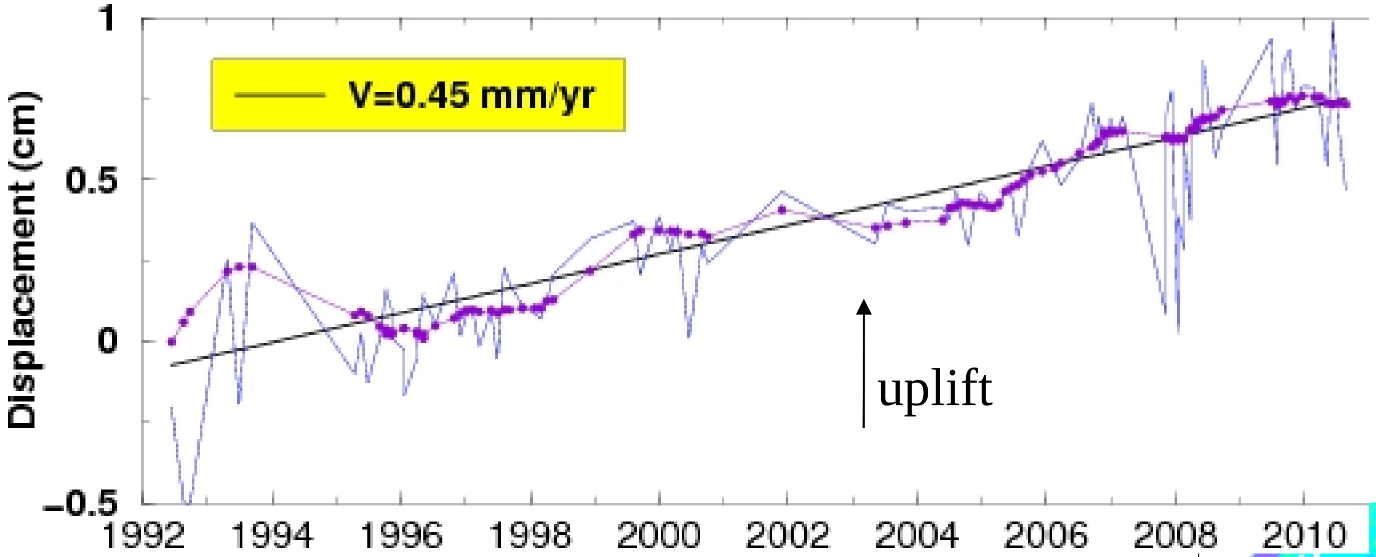

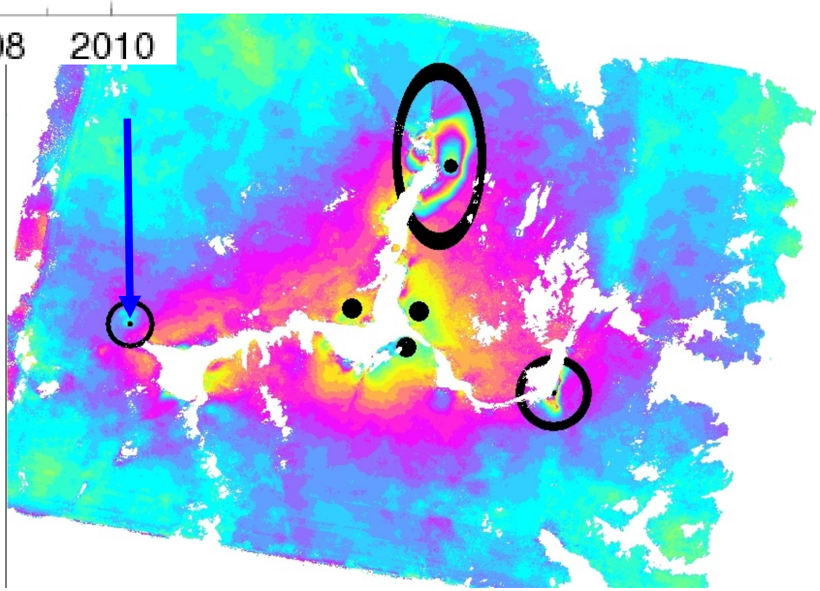

Regression coefficient between data and lake level

Effect of water load fluctuations

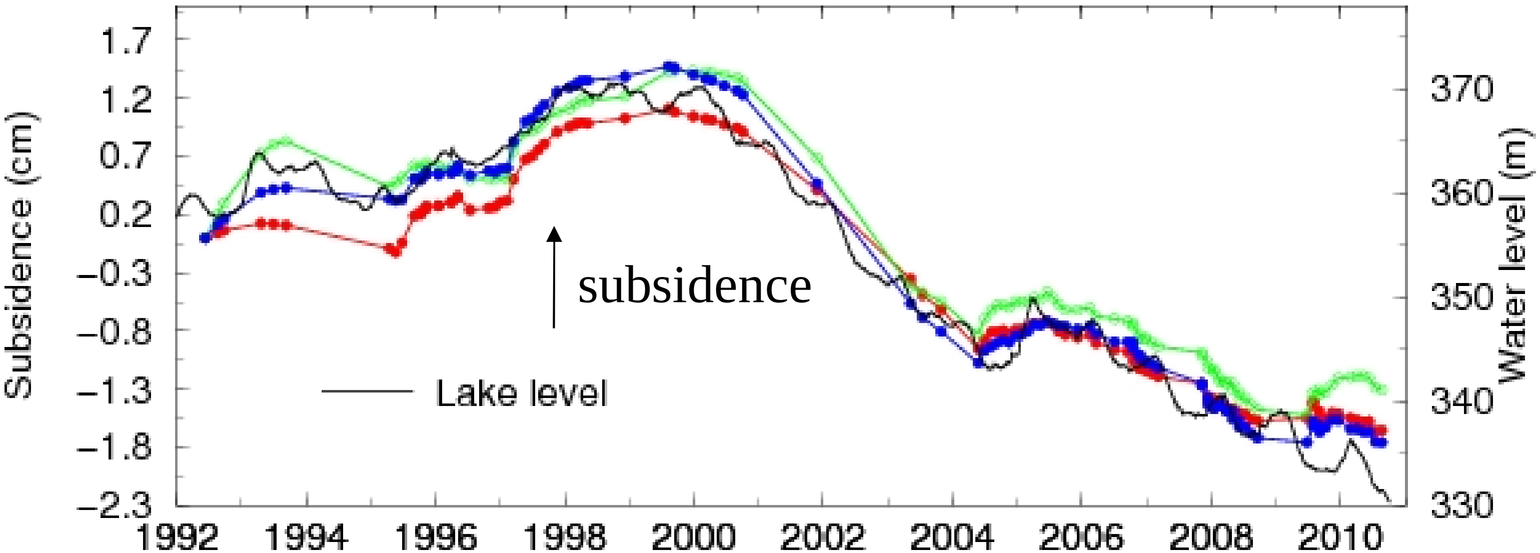

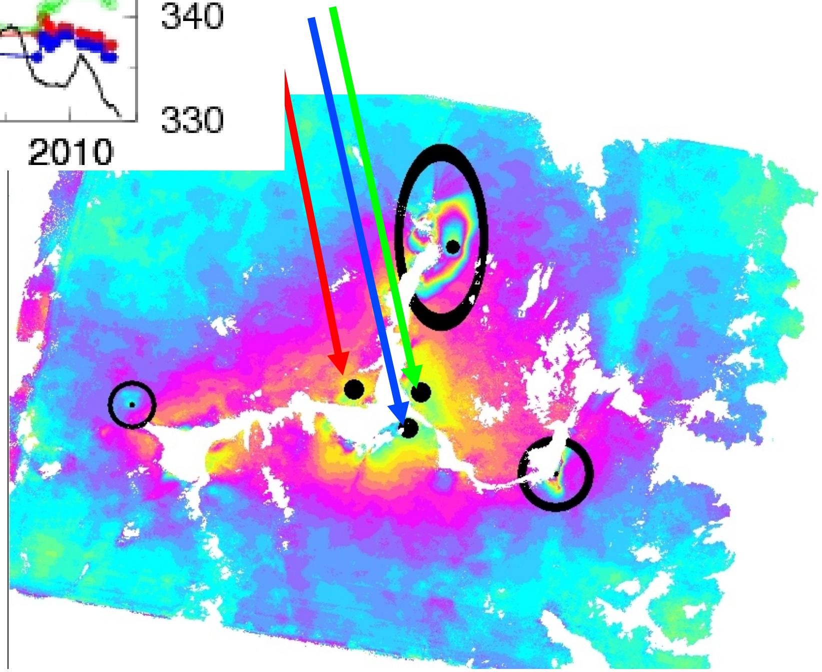

Very good correlation between load and ground motion : elastic ?

Regression coefficient between data and lake level

Modeling Forward predictions :

Layered Maxwell compressible viscoelastic model

* Elastic model, constrained from Vp and Vp/Vs
  32 km crust : $\lambda = 36.5$ GPa, $\mu = 35.5$ GPa
  uniform uppermost mantle : $\lambda = 72.6$ GPa, $\mu = 64.1$ Gpa

* Viscoelastic model
  same elastic structure
  uppermost mantle viscosity of 10^{18} Pa.s, elastic thickness of 32 km
  (Kaufmann and Amelung, 2000)

Comparison with elastic and visco-elastic models

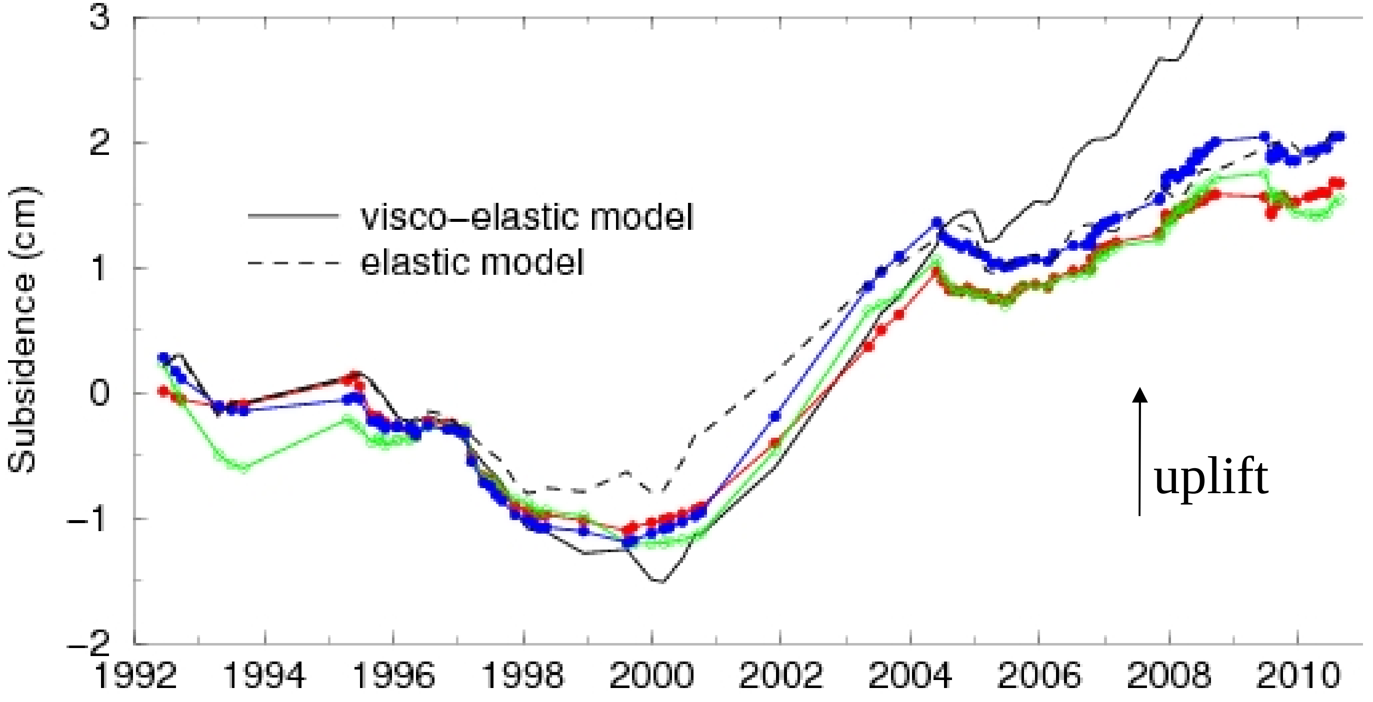

1992-2002 : follows the visco-elastic model
2004-2010 : follows the elastic model
==> exclude the viscosity of 10^{18} Pa.s

Conclusion :

♦ Detect transient sub-centimeter ground motions associated with water level fluctuations

● At a small spatial scale (10x20 km^2 or less), clear delayed poro-elastic response of sedimentary layers to water level fluctuations. WELL DEFINED !

● At large spatial scale (~ 100 x 100 km^2), clear ground motion response to lake load variations.

▶ Results are sensitive to the phase/elevation correction (atmospheric moisture)

▶ Large scale atmospheric patches decrease the time series accuracy

♦ We now clearly exclude the viscosity structure given by Kaufmann and Amelung, although it provides a good fit to the 1992-2001 data.
==> Characterize the shape (G(x,y)F(t)) of the “non-elastic” signal ?

Atmospheric delays (e.g., Hanssen, 2001):

$$\text{Delay (m)} = 10^{-6} \int \left(k_1 \frac{P}{T} + k_2 \frac{e}{T} + k_3 \frac{e}{T^2} + k_4 W_{cl} - k_5 \frac{n_e}{f^2} \right) dz$$

Dry delay
~ 2.3 m

Wet delay
~ 0.3 m

Liquid delay
~ 4 mm

Ionosphere,
dispersive, ?

DInSAR :

* blind to absolute delay
* sees variations both in space and time (double differences)

Two main effects :

* Changes in atmospheric vertical stratification : leads a delay correlated with elevation
* Atmospheric turbulence : random spatial patterns

Phase-elevation correlation : comparison with predictions derived from the North American Regional Analysis

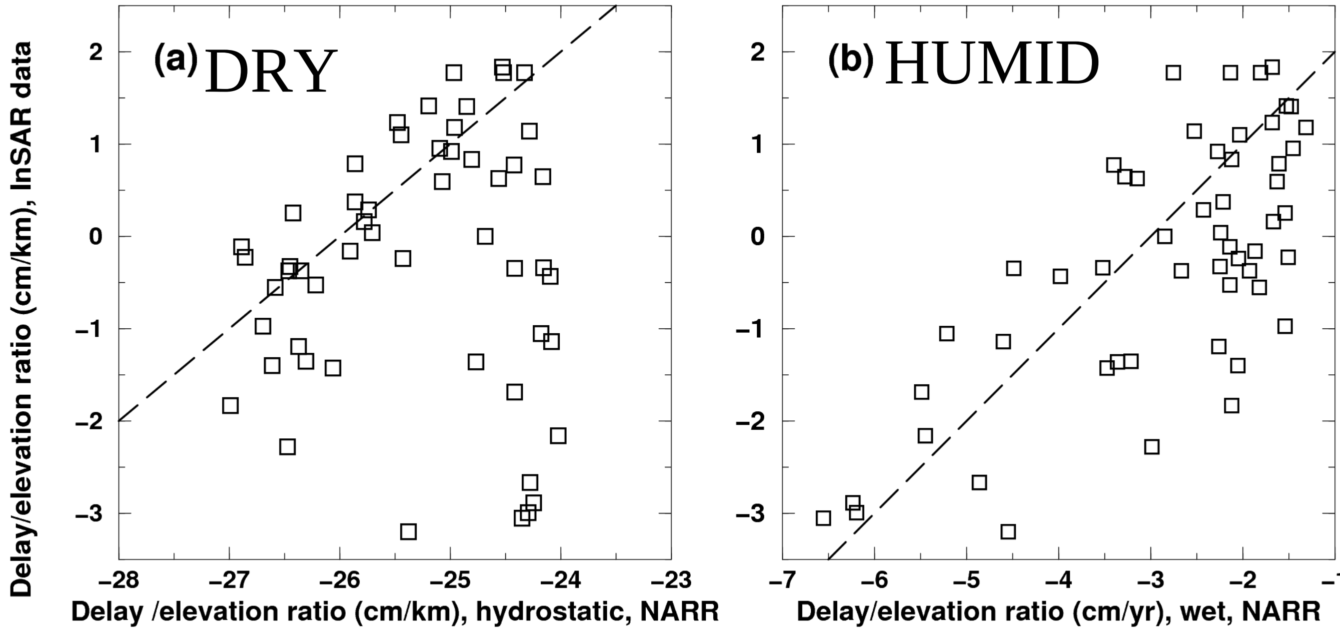

COMPARISON
DInSAR
versus
NARR prediction

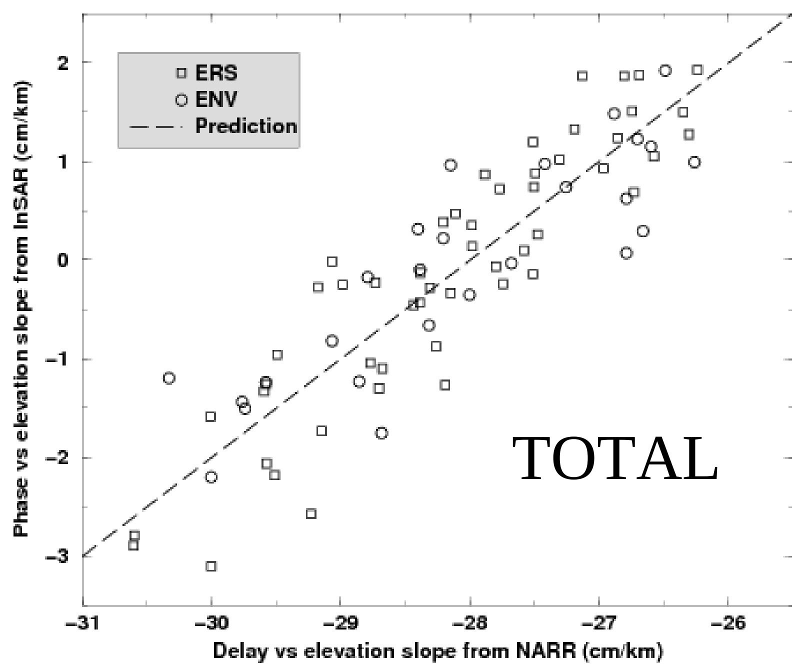

Doin et al.,
J. of Applied
Geophys., 2009

Spatial comparison using Principal Component Analysis

First eigen vector:

On raw phase delays

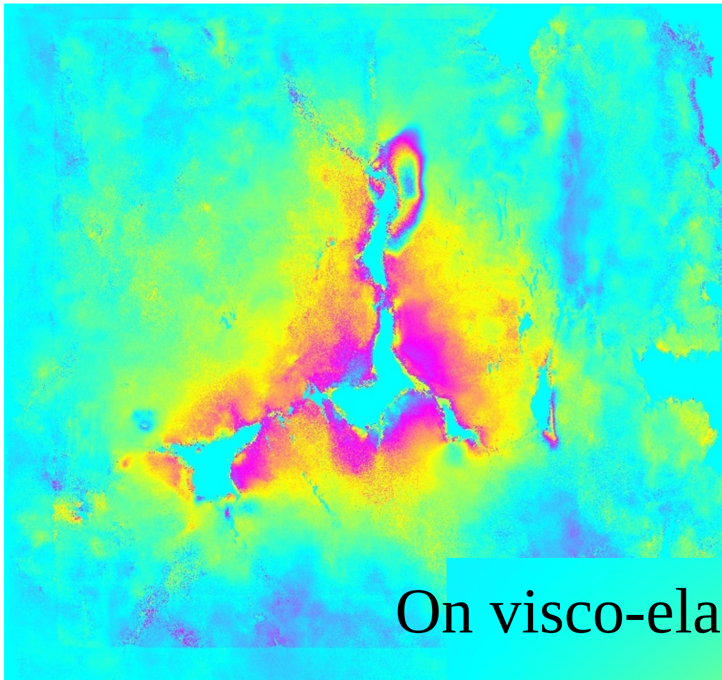

On elastic model evolution

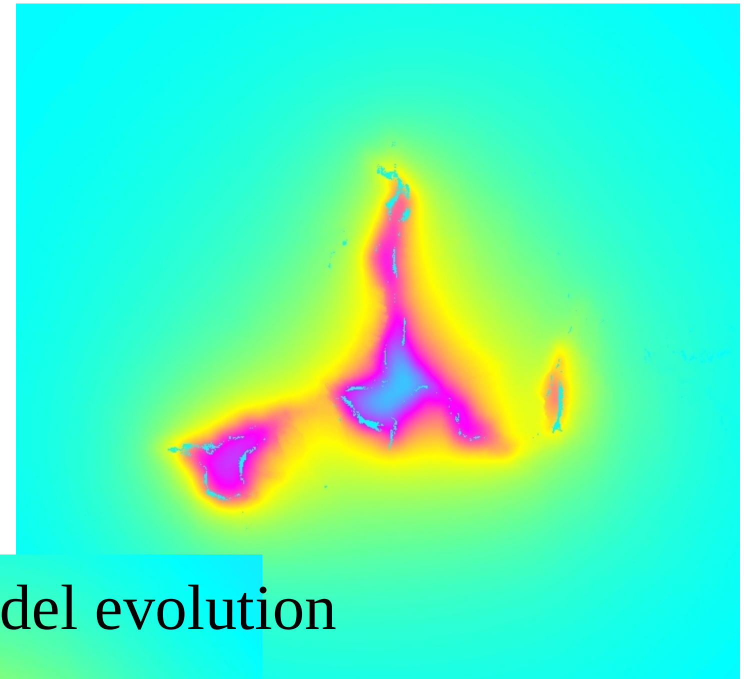

On visco-elastic model evolution

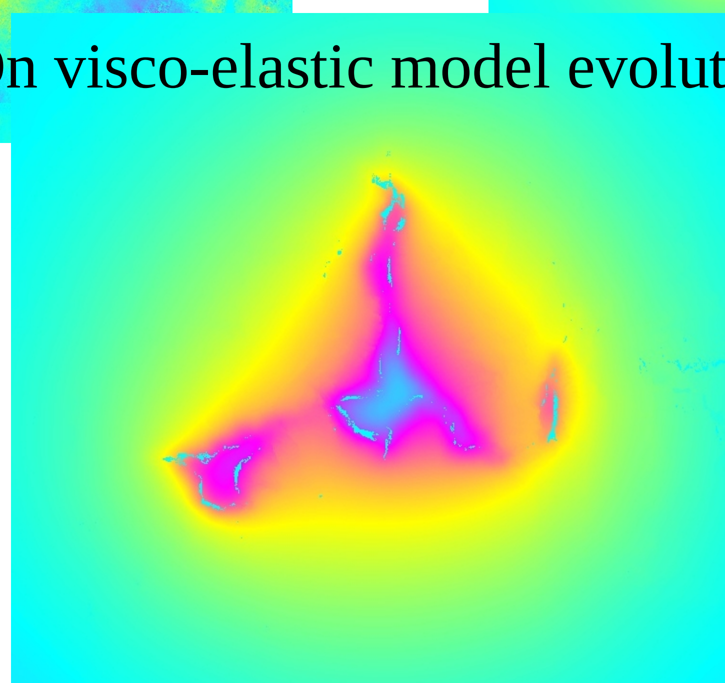

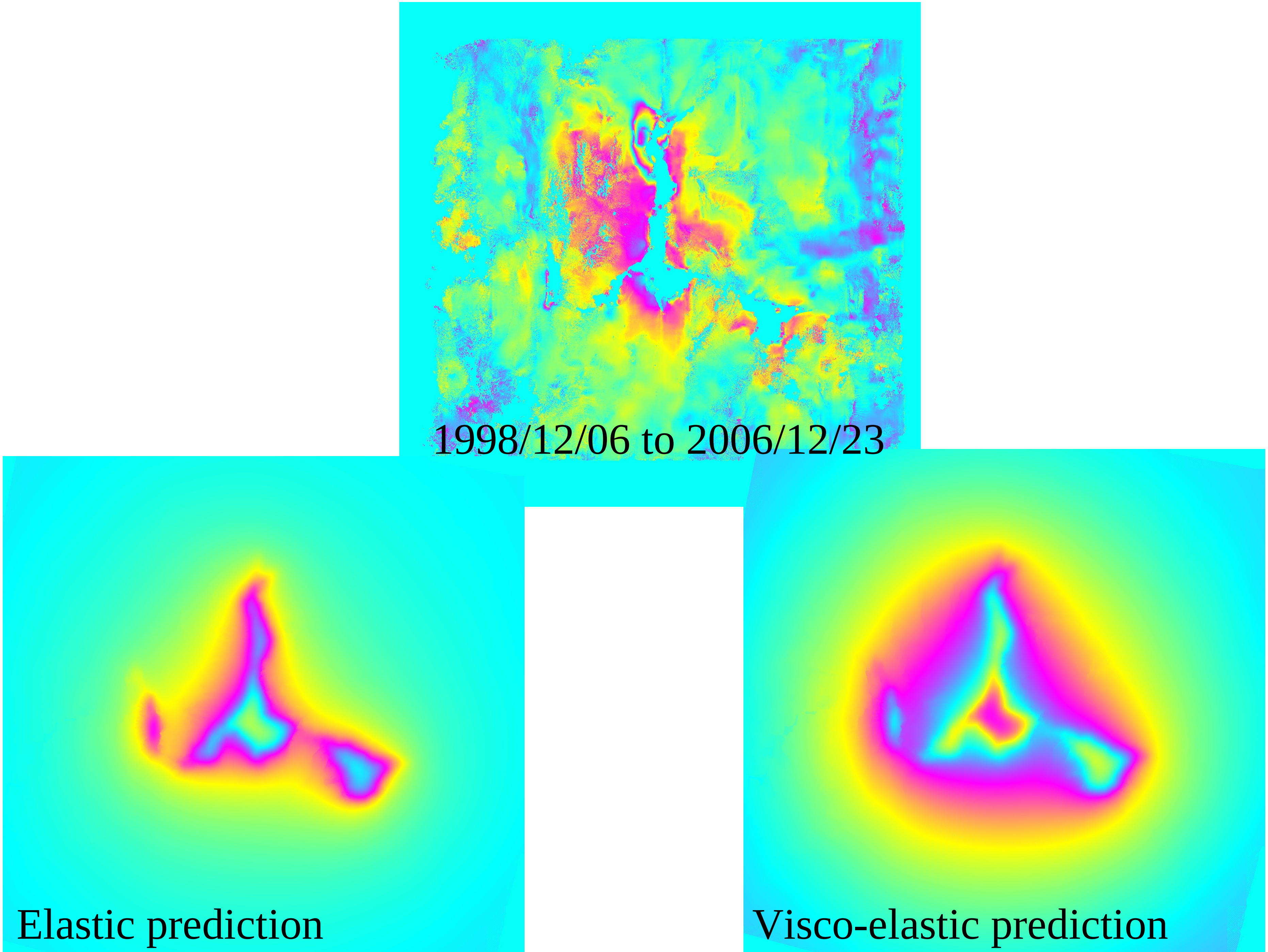
1998/12/06 to 2006/12/23
Elastic prediction
Visco-elastic prediction

Inversion of interferograms into time series

- Effect of smoothing

Correlation of LOS displacement with lake level variations

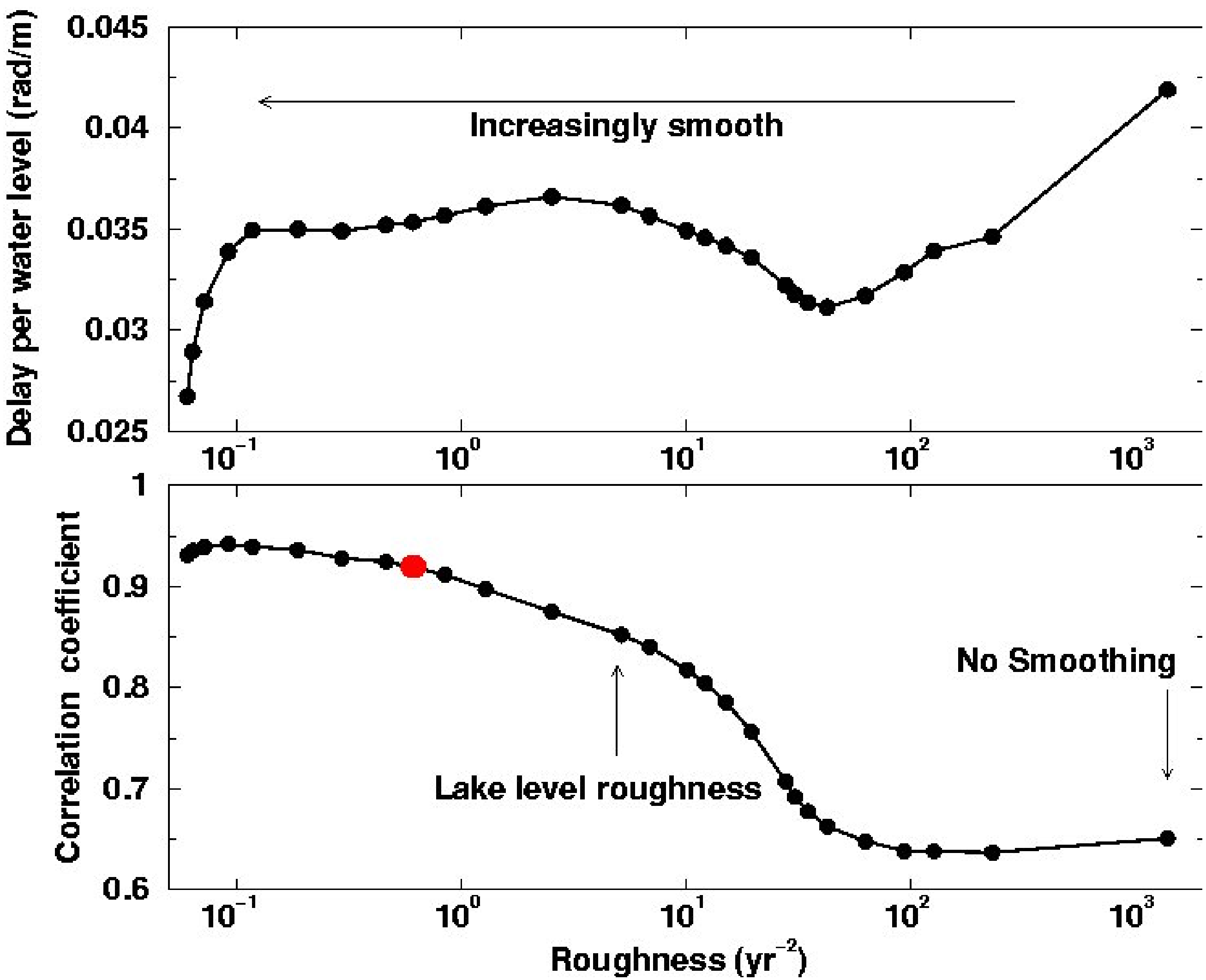

Viscoelastic model

Elastic model

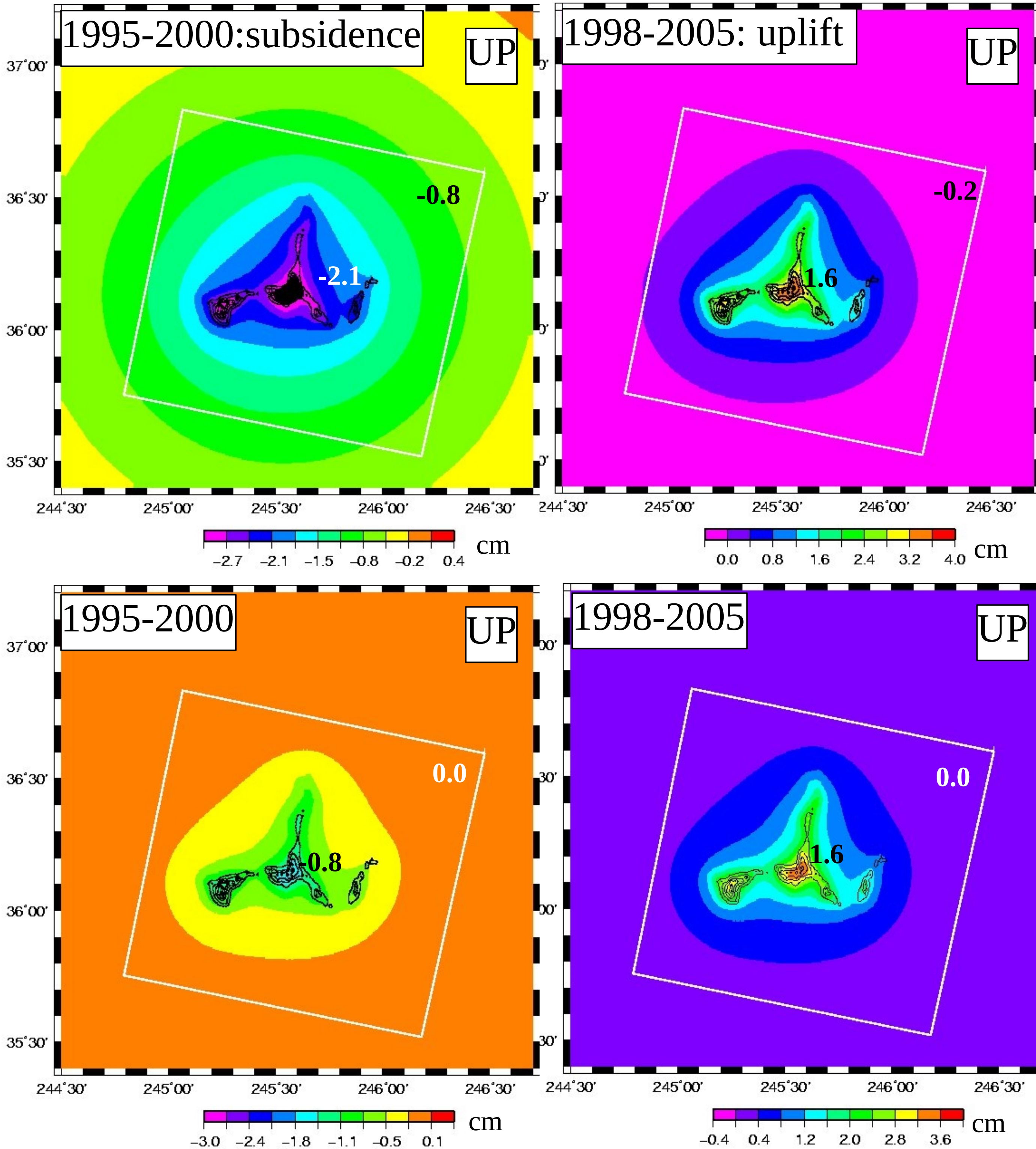

Comparison with forward elastic and visco-elastic models

Comparison between data stack and model stacks

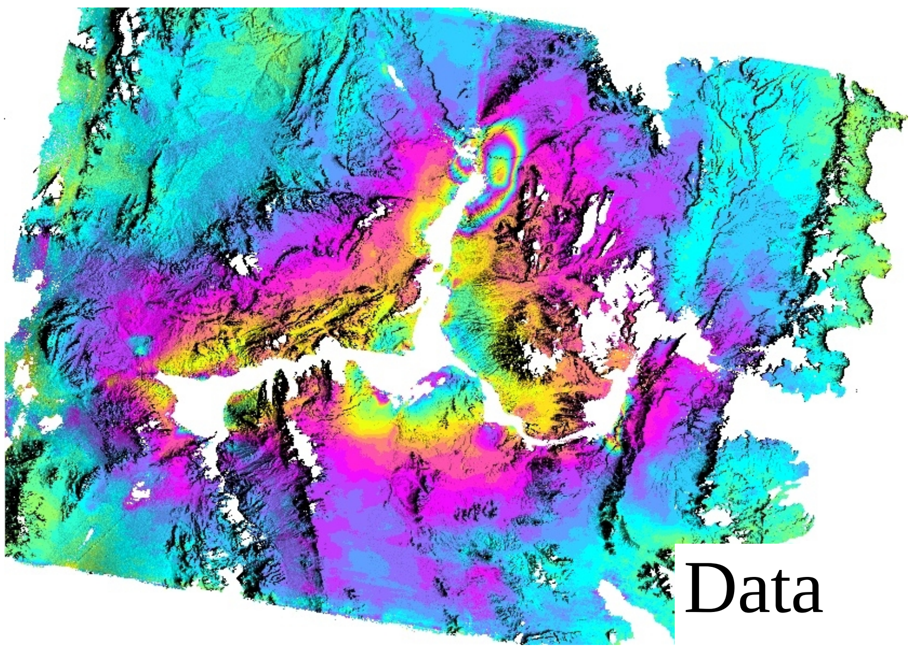

Data

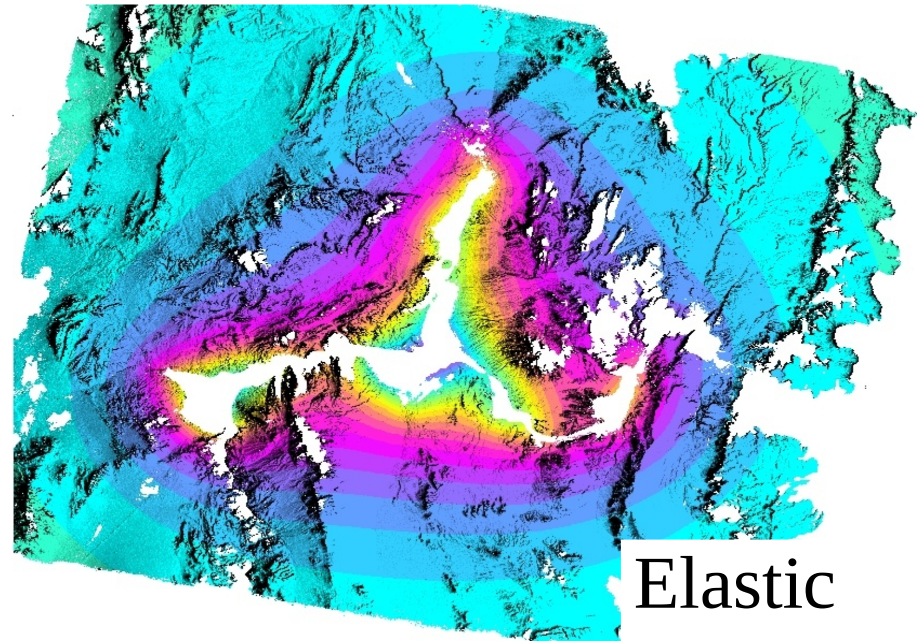

Elastic

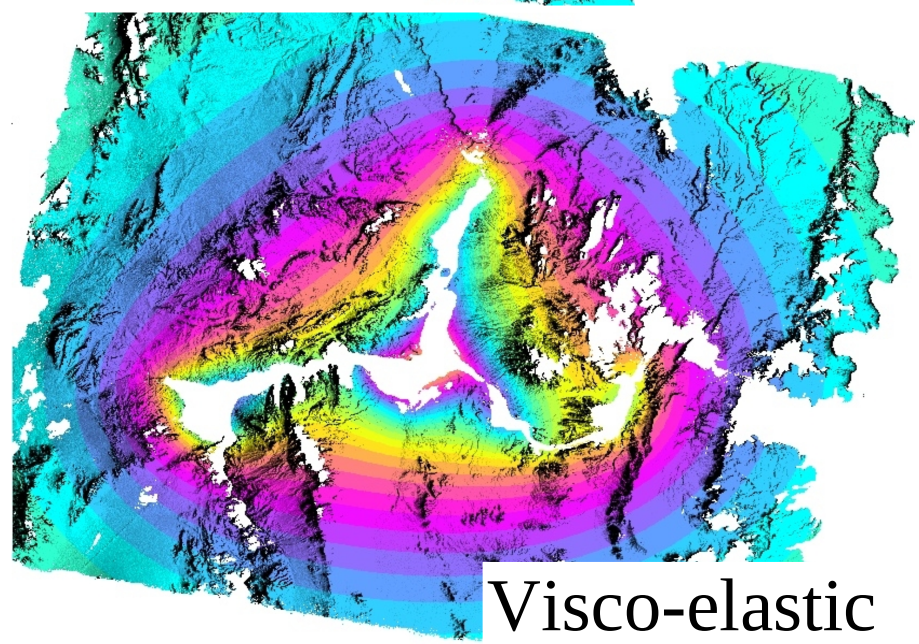

Visco-elastic

Comparison with forward elastic and visco-elastic models

Residues

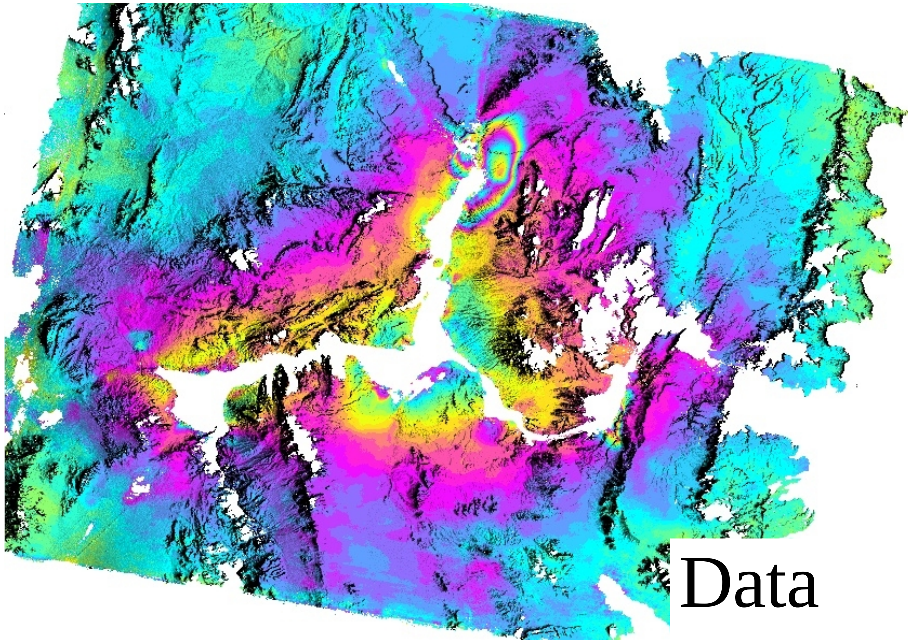

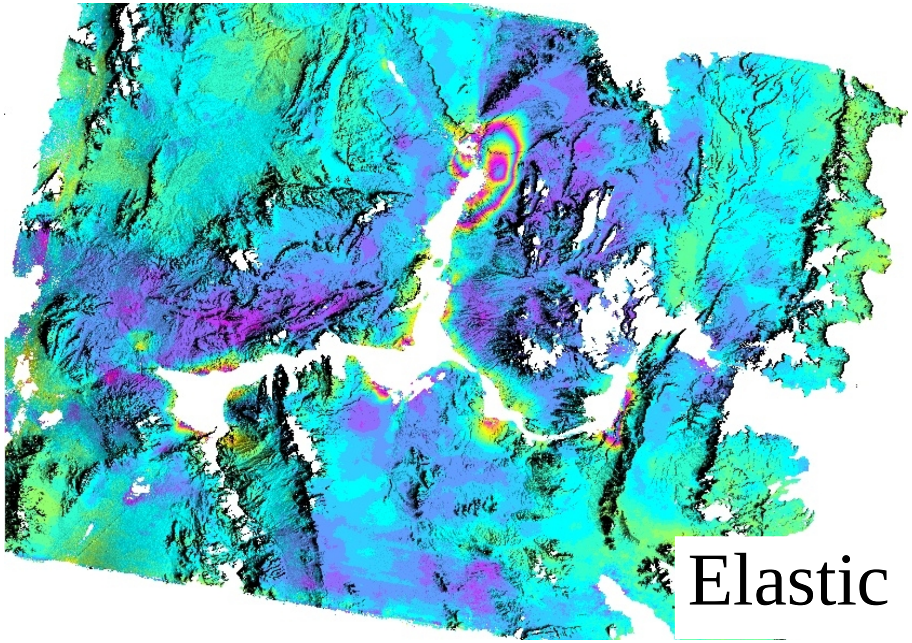

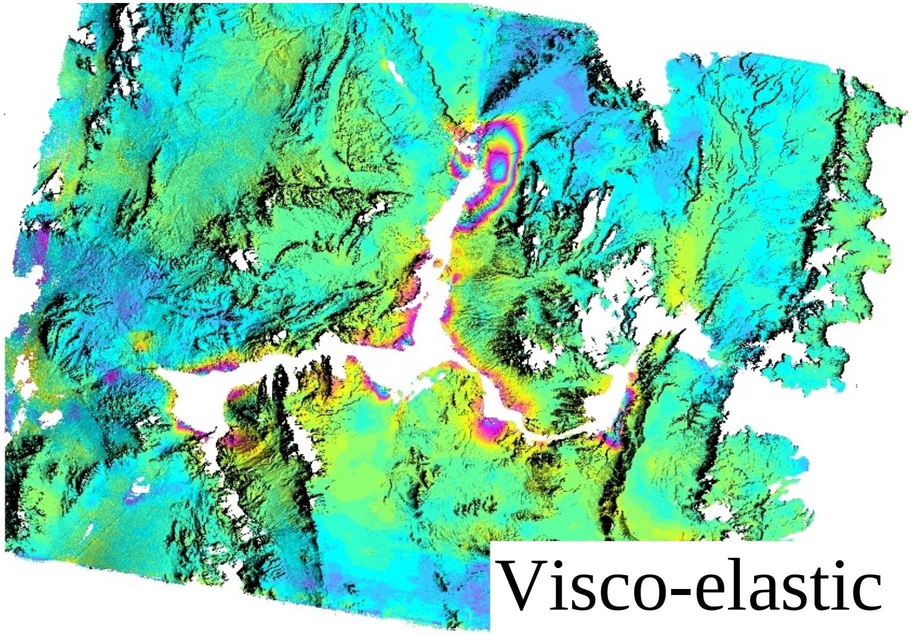

In between the two models ?
Larger viscosity than inverted by K&A ?

SAR data : 63 ERS acquisitions, 45 Envisat acquisitions analysed with a Small BASeline approach (Schmidt and Bürgmann, 2003)

pre-2001 to post-2003 links

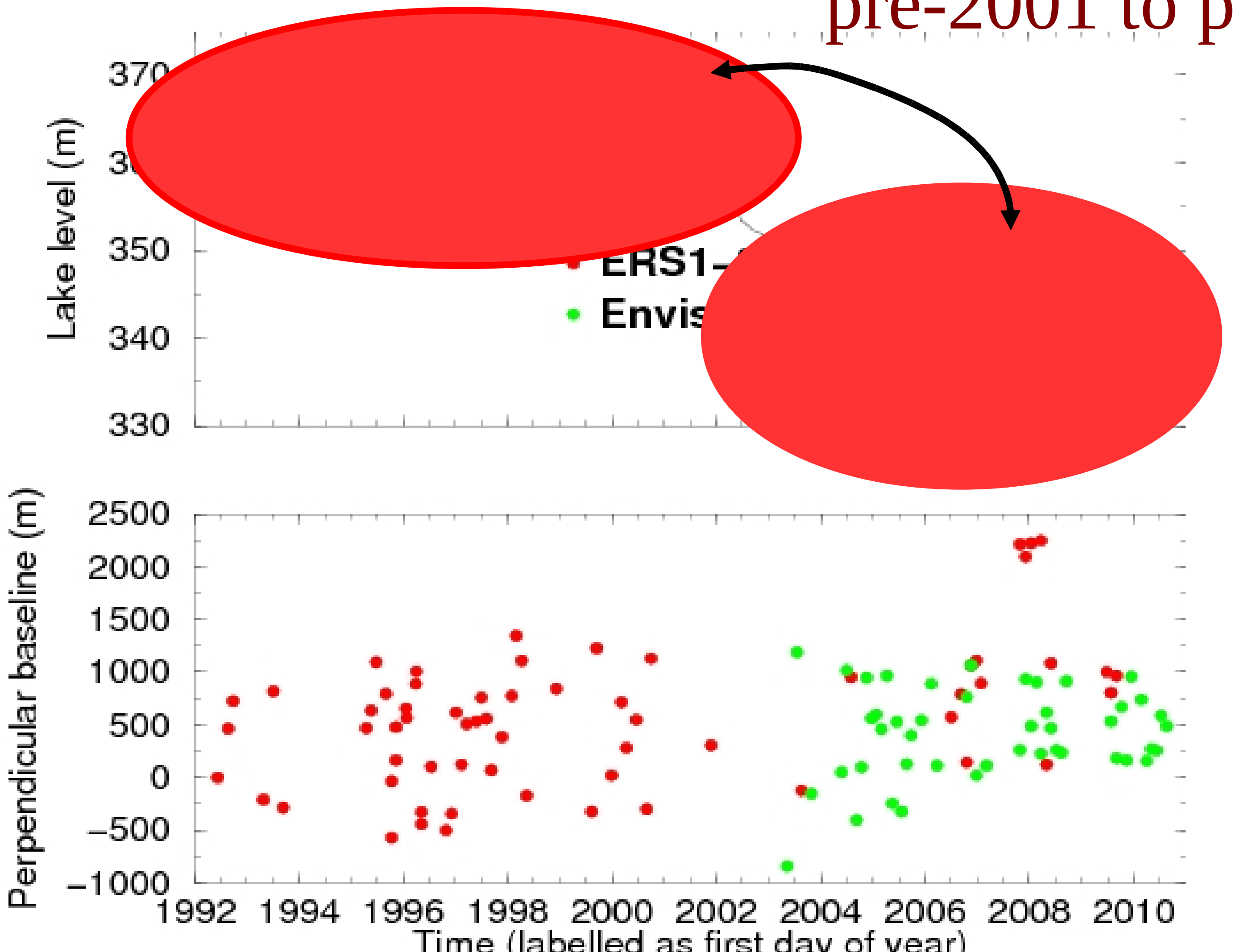

ERS2 post-2000 images

squint angle variations : small overlap in doppler frequency in azimuth

Amplitude of random patterns for each acquisition

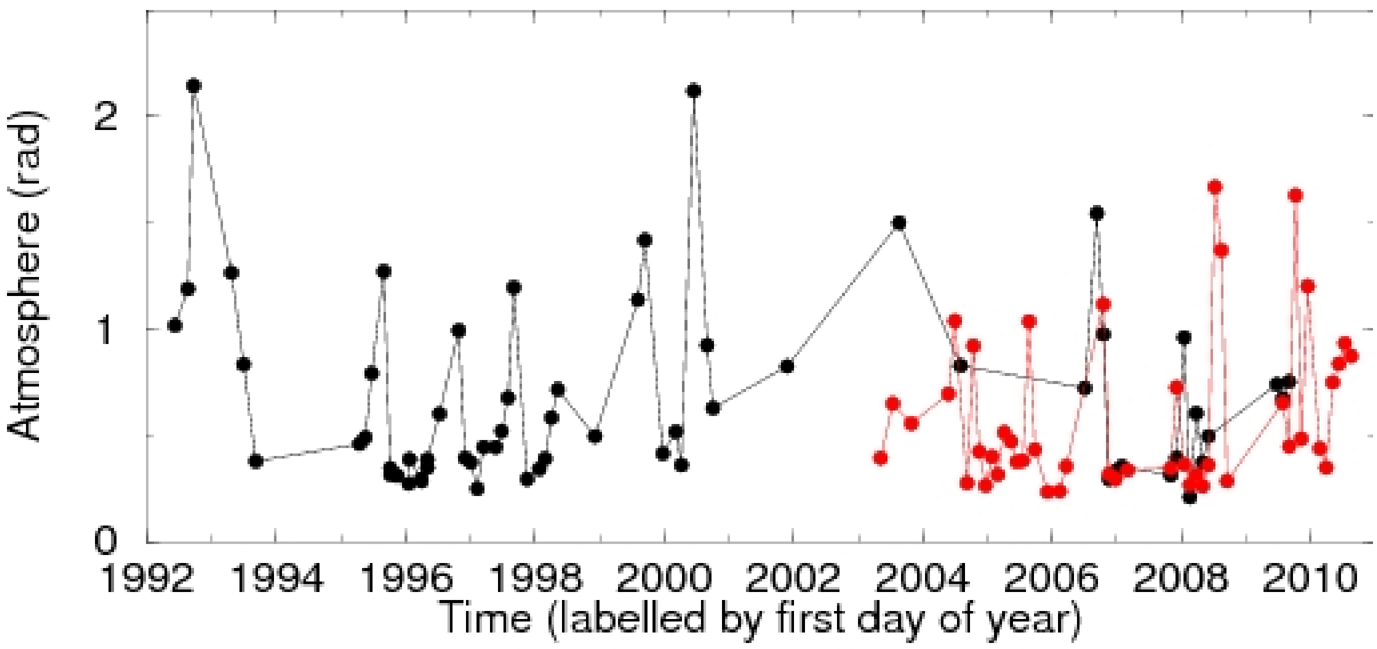

Monsoon episodes
during summer with a strong
atmospheric turbulence